

Review

The Hunt for Supersymmetry at the Tevatron

André Sopczak

Institute of Experimental and Applied Physics, Czech Technical University in Prague, Horska 3a, CZ-12800 Prague 2, Czech Republic; E-Mail: andre.sopczak@cern.ch

Received: 30 December 2013 / Accepted: 17 February 2014 / Published: 19 March 2014

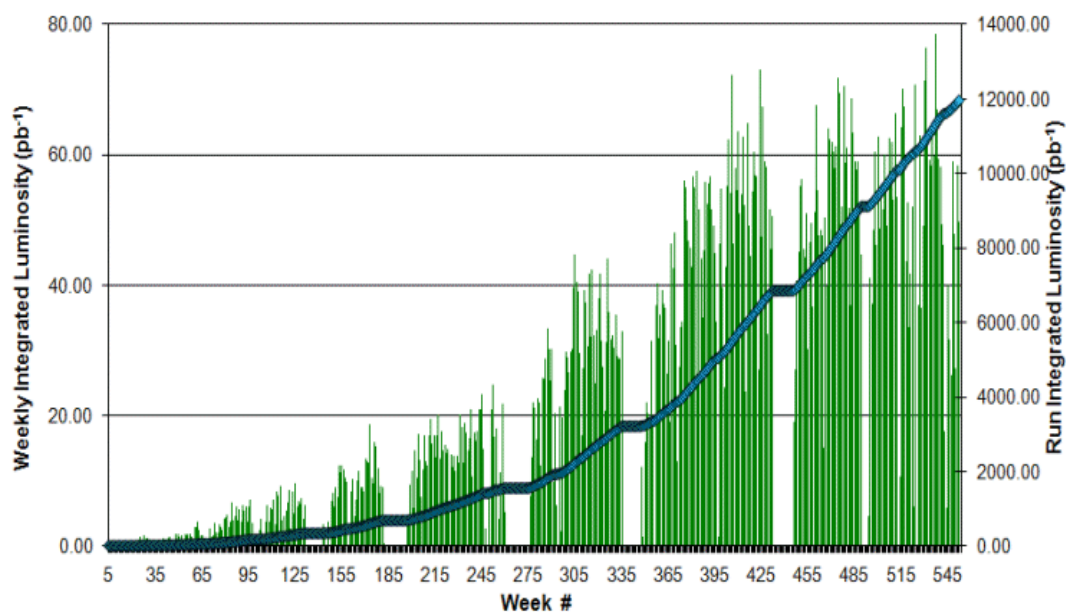
Abstract: During the Tevatron data-taking period from April 2001 to September 2011 (Run-II), several searches for supersymmetric particles were performed. The results from searches by the CDF and DØ collaborations are concisely reviewed. This includes results up to the summer conferences of 2013. Model-independent and model-dependent limits on new particle production are set, and interpretations in supersymmetric models are given. Several limits from the Large Electron Positron (LEP) era have been extended. Specific results are placed into the context of the Tevatron performance expectations and a few of the current results from searches at the Large Hadron Collider (LHC).

Keywords: supersymmetry; Tevatron; CDF; DØ

1. Introduction

The search for supersymmetric particles was pioneered at the Super Proton Synchrotron (SPS) and Large Electron Positron (LEP) colliders at CERN (Conseil Européen pour la Recherche Nucléaire) and has been extensively advanced at the Tevatron (chiefly Run-II with data taken 2001–2011). A wide range of analyses is presented, illustrating major improvements in the analysis sensitivities. This review is not inclusive of all searches for supersymmetric particles, but rather, is intended to give an overview of several important results and relating them to the underlying theoretical framework. For details of specific experimental analysis techniques and the event selections of the individual search channels, the reader is referred to the publications by the CDF and DØ collaborations. After the first few years of data-taking with rather low instantaneous luminosity, the Tevatron collider achieved significantly higher collision rates in the second half of Run-II. The total delivered luminosity is about 12 fb^{-1} , of which about 10 fb^{-1} were recorded by each experiment. Figure 1 [1] shows the delivered Run-II luminosity between 2001 and 2011.

Figure 1. Delivered Tevatron luminosity (data-taking period: April 2001 to September 2011) [1].



The discovery of a supersymmetric particle would extend the Standard Model (SM) of particle physics and lead the way to a new level of understanding of the fundamental elements of our Universe.

Supersymmetric particle searches at the Tevatron are reviewed for di-photon signatures in the gauge-mediated supersymmetry breaking (GMSB) interpretation (Section 2.1), tri-lepton signatures (Section 2.2), gluinos and scalar quarks (Section 2.3), scalar tops (Section 2.4), scalar bottoms (Section 2.5) and charged massive particles (Section 2.6). In Section 3, first, LHC results [2] are compared with the Tevatron results, and a brief outlook is given. An overview of the reviewed analyses is given in the Appendix A.

2. Supersymmetric Particle Searches at the Tevatron

In the production of supersymmetric particles (sparticles), the lightest supersymmetric particle (LSP) is stable (if the so-called R-parity is conserved) and escapes detection, leading to missing momentum and missing energy in the recorded events. Examples of such events are shown in Figure 2 [3–5]. The events reported by the $D\bar{0}$ and CDF collaborations have jets and large missing energy (for $D\bar{0}$ [3,4], large H_T is defined as the sum of the transverse jet momenta, and for CDF [5], it is defined as the sum of the transverse jet energies).

Previous combined results from the LEP experiments have set limits on several sparticles with masses close to the kinematic reach. Figure 3 [6] shows the excluded region in the $\tan\beta$ versus LSP mass plane in the Minimal Supersymmetric extensions of the Standard Model (MSSM) and in the Gauge Mediated Symmetry Breaking (GMSB) model. The position in the GMSB parameter space of an intriguing CDF $e\bar{e}\gamma\gamma$ candidate from the Tevatron Run-I is indicated (dashed line) [7]. The GMSB interpretation for this event was later excluded at 95% Confidence Level (CL) by the LEP experiments.

Figure 2. Examples of events with large missing momentum and energy. The tracks result from charged particles produced at the interaction point. The height of the towers indicates the energy deposited in the calorimeters. In the CDF event display, the arrow indicates the direction of the missing momentum. (a) DØ $H_T = 410$ GeV [3]; (b) CDF $H_T = 404$ GeV [5].

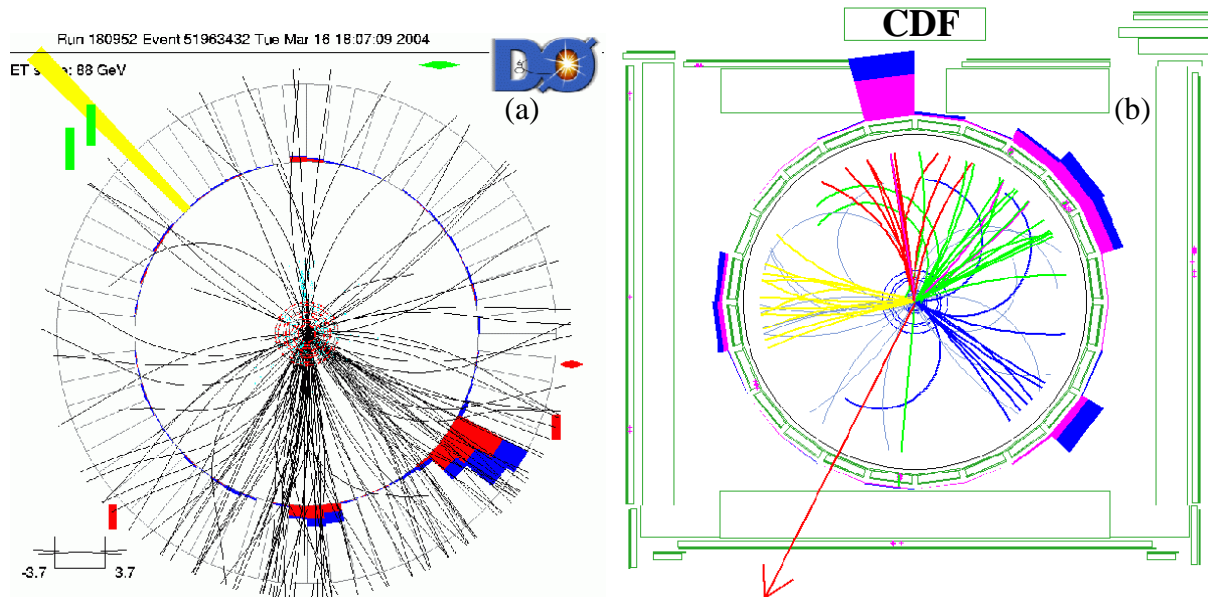
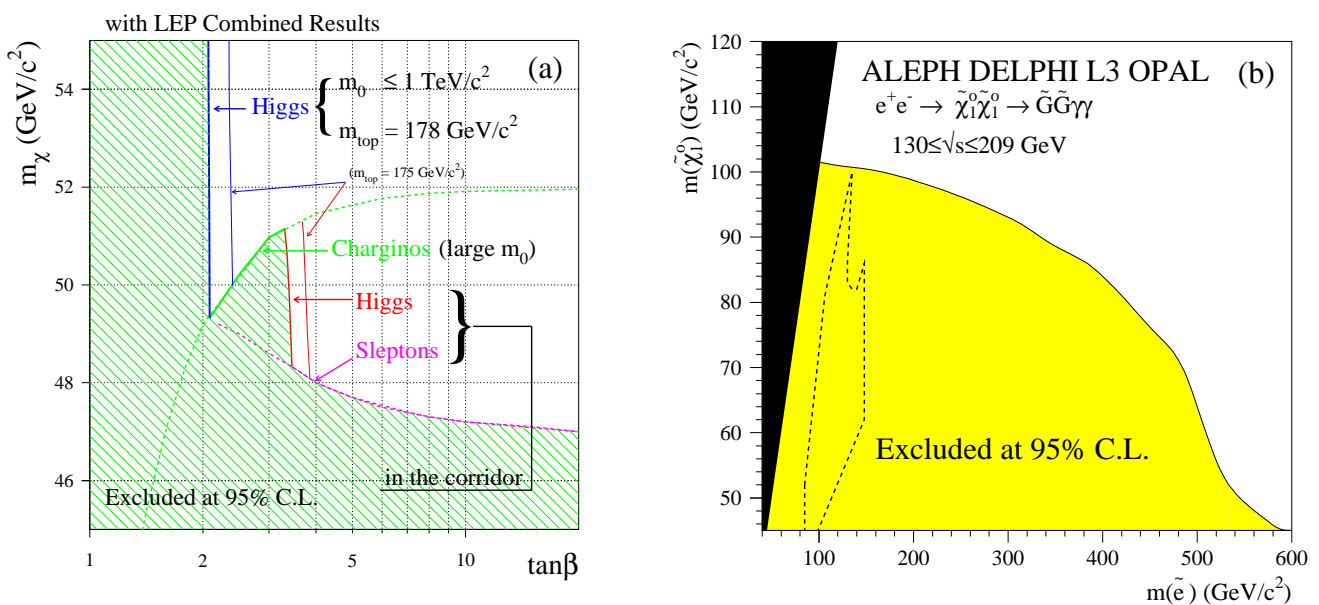


Figure 3. (a) Combined LEP limits in the $(\tan \beta, \text{neutralino mass})$ plane in a constrained MSSM [6]; (b) Combined LEP exclusion in the $(\text{selectron mass, neutralino mass})$ plane from acoplanar photon searches [6]. The CDF Run-I $e\bar{e}\gamma\gamma$ candidate event is indicated in the excluded region [7].



2.1. Di-Photon (GMSB Interpretation)

In the GMSB model, chargino-neutralino production has been searched for by the CDF and DØ collaborations. In the GMSB model, the lightest neutralino, $\tilde{\chi}_1^0$, is the Next-to-Lightest Supersymmetric Particle (NLSP) and decays to a gravitino, \tilde{G} , and a photon. In this model, the LSP is the gravitino, which is a very light and weakly interacting particle. The production reaction is illustrated in Figure 4. The expected signal can be well separated from the background events [8]. There is no indication of a signal in the early data, and combined limits on the chargino mass from CDF [9] and DØ [8] were given [10]. Large progress has been made in recent years, and the results using 6.3 fb^{-1} for DØ and 2.6 fb^{-1} for CDF are shown in Figures 5 [11] and 6 [12]. The experimental sensitivity on the production cross-section at 95% CL is now, below 7 fb. As a result, in the SPS8 (Snowmass Points and Slopes, parameters in scenario 8) benchmark, the DØ collaboration excluded an effective Supersymmetry breaking scale below 124 TeV at 95% CL, as well as the lightest neutralino and lightest chargino masses below 175 GeV and 330 GeV, respectively. A search for a long-lived particle that decays into a pair of photons resulted in a 95% CL lower mass limit of 101 GeV on the lightest neutralino at a 5-ns lifetime [13]. Recently, updated results for searches for massive, long-lived particles that decay to photons in the exclusive photon and missing energy final state have been reported by the CDF collaboration [14]. Figure 7 shows a simulated signal and the experimental measurement. No indication of a signal is observed.

Figure 4. Production graph for DØ GMSB di-photon searches.

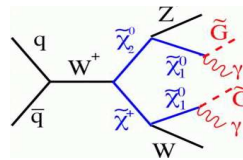


Figure 5. DØ GMSB di-photon, copyright (2010), with permission by the American Physical Society [11]. (a) Missing transverse energy; (b) The limit at 95% CL for the SPS8 (Snowmass Points and Slopes) benchmark parameter scenario.

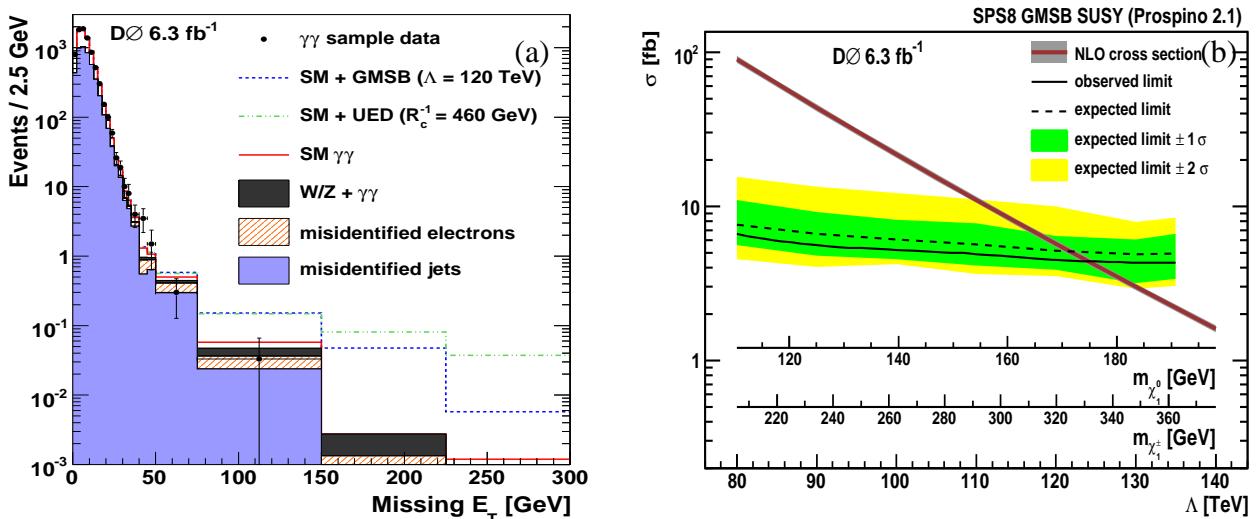


Figure 6. CDF GMSB di-photon searches, copyright (2010), with permission by the American Physical Society [12]. (a) Missing transverse energy and H_T ; (b) The limit at 95% CL. For a neutralino lifetime above about 1.5 ns, the sensitivity decreases.

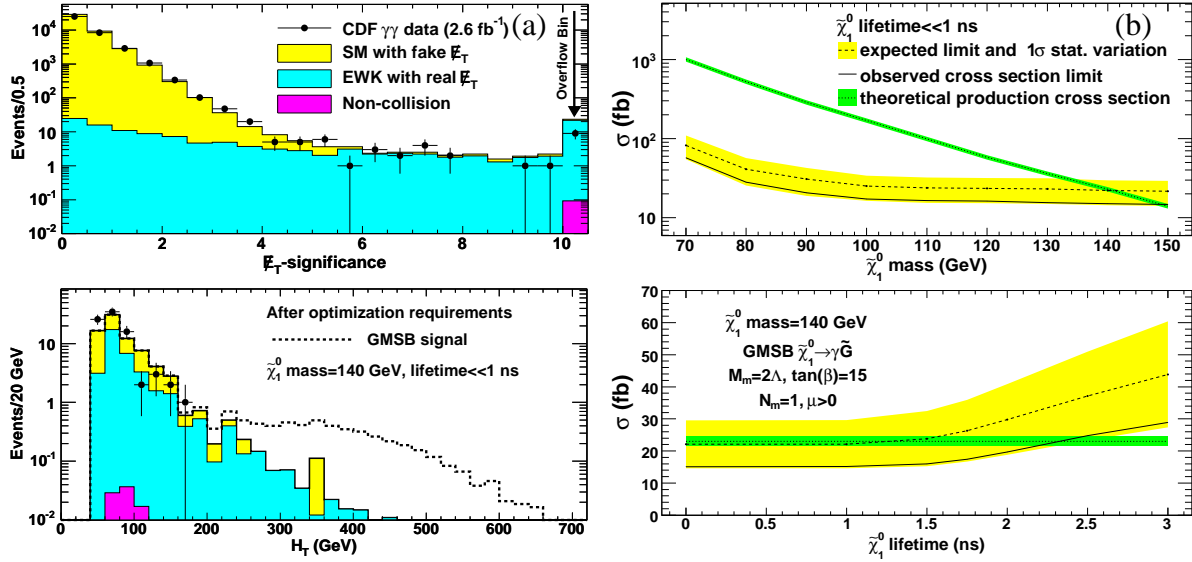
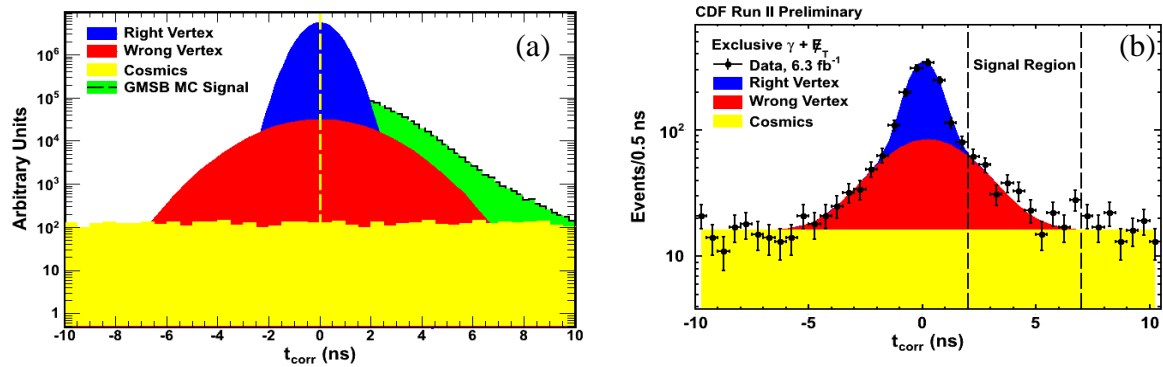


Figure 7. CDF delayed photon searches [14]. (a) Expected timing distribution divided into components. Standard model backgrounds contribute right and wrong vertex Gaussians and cosmics contribute a flat background. The signal from a long-lived neutralino would look approximately like a falling exponential smeared by the detector resolution; (b) Measured timing distribution with the best fit of the backgrounds.



2.2. Tri-Lepton Signatures

The sparticle production with a tri-lepton final state is illustrated in Figure 8. This scenario is called ‘‘Supersymmetry golden mode’’ because of the small expected background level. As an example, Figure 9a shows early results for the $\mu\mu\ell$ final state [15–18]. Furthermore, the other tri-lepton final states ($e\mu\ell$, $e\ell\ell$, $e\tau$, $\mu\tau$) were studied. Good agreement between data and simulated background for the various final states with tri-lepton signatures was observed. The data does not show any indication of a supersymmetric signal above the background.

With increasing luminosities, the expectations from 2005 for the chargino mass reach were 170, 210, 235 and 265 GeV with one, two, four and 8 fb⁻¹, respectively, for a scenario with a maximal leptonic branching ratio, as shown in Figure 9b [19].

Examples of the updated DØ results with 2.3 fb⁻¹ are shown in Figure 10 [20] and CDF results in Figure 11 [21,22]. With 5.8 fb⁻¹ CDF data, a chargino mass below 168 GeV is excluded at 95% CL in the minimal SuperGRAvity (mSUGRA) model. The CDF collaboration also searched for final states involving tau leptons. Results from these searches are shown in Figures 12 and 13 [23,24].

Figure 8. Production graph for DØ tri-lepton searches.

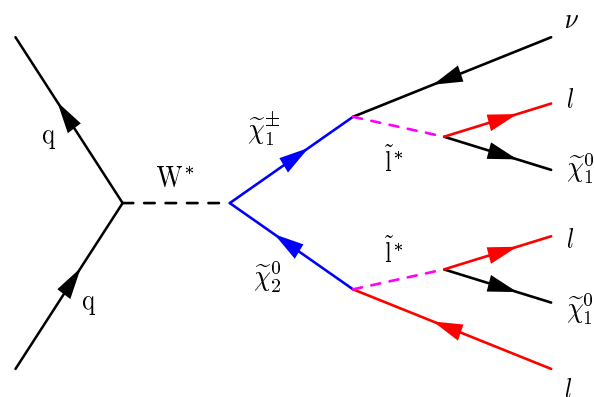


Figure 9. DØ tri-lepton searches. (a) Invariant di-muon mass $m_{\mu\mu}$, copyright (2005), with permission by the American Physical Society [18]; (b) Sensitivity expectations from 2005 for the tri-lepton searches with larger luminosities [19].

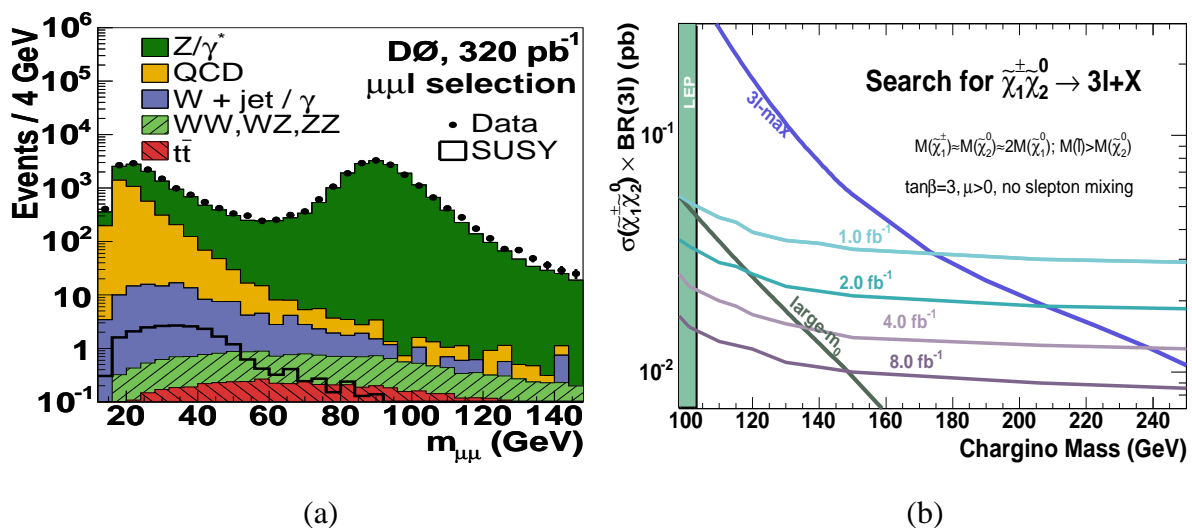


Figure 10. DØ tri-lepton searches [20]. (a) The upper limit at the 95% CL on $\sigma \times \text{BR}(3\ell)$ as a function of the $\tilde{\chi}_1^\pm$ mass from the tri-lepton searches and expectations for two Supersymmetry scenarios (3 ℓ -max and large m_0); (b) The region in the m_0 - $m_{1/2}$ plane excluded by the combination of the DØ analyses (green), by LEP searches for charginos (light grey) and sleptons (dark grey) [6] and CDF searches based on 2.0 fb⁻¹ data (black line) [21,22]. The assumed mSUGRA parameters are $\tan\beta = 3$, $A_0 = 0$ and $\mu > 0$; (c) The upper limit at the 95% CL on $\sigma \times \text{BR}(3\ell)$ as a function of $\tan\beta$ and a prediction for a chargino mass of 130 GeV with $m_{\tilde{\tau}} - m_{\tilde{\chi}_2^0} = 1$ GeV.

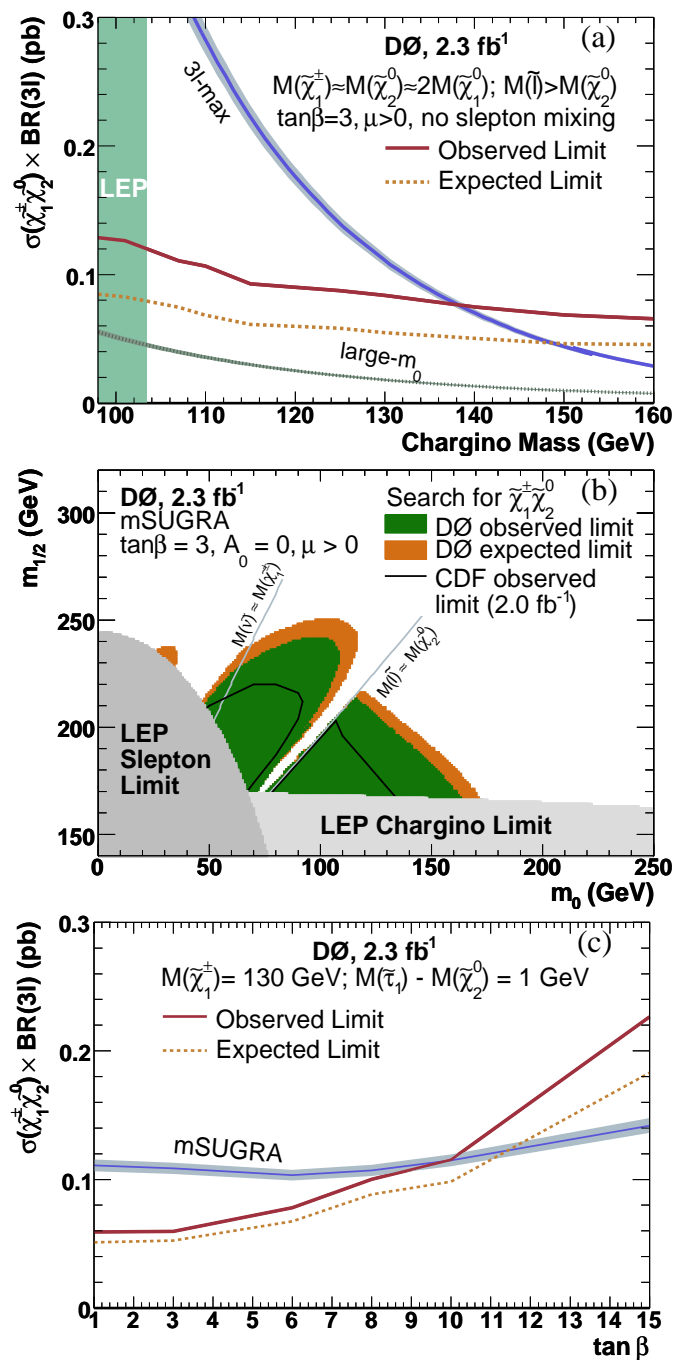


Figure 11. CDF tri-lepton searches in the $\mu\mu$ channel [21,22]. (a) Invariant mass; (b) Missing E_T ; (c) The limit from ee and $\mu\mu$ channels combined.

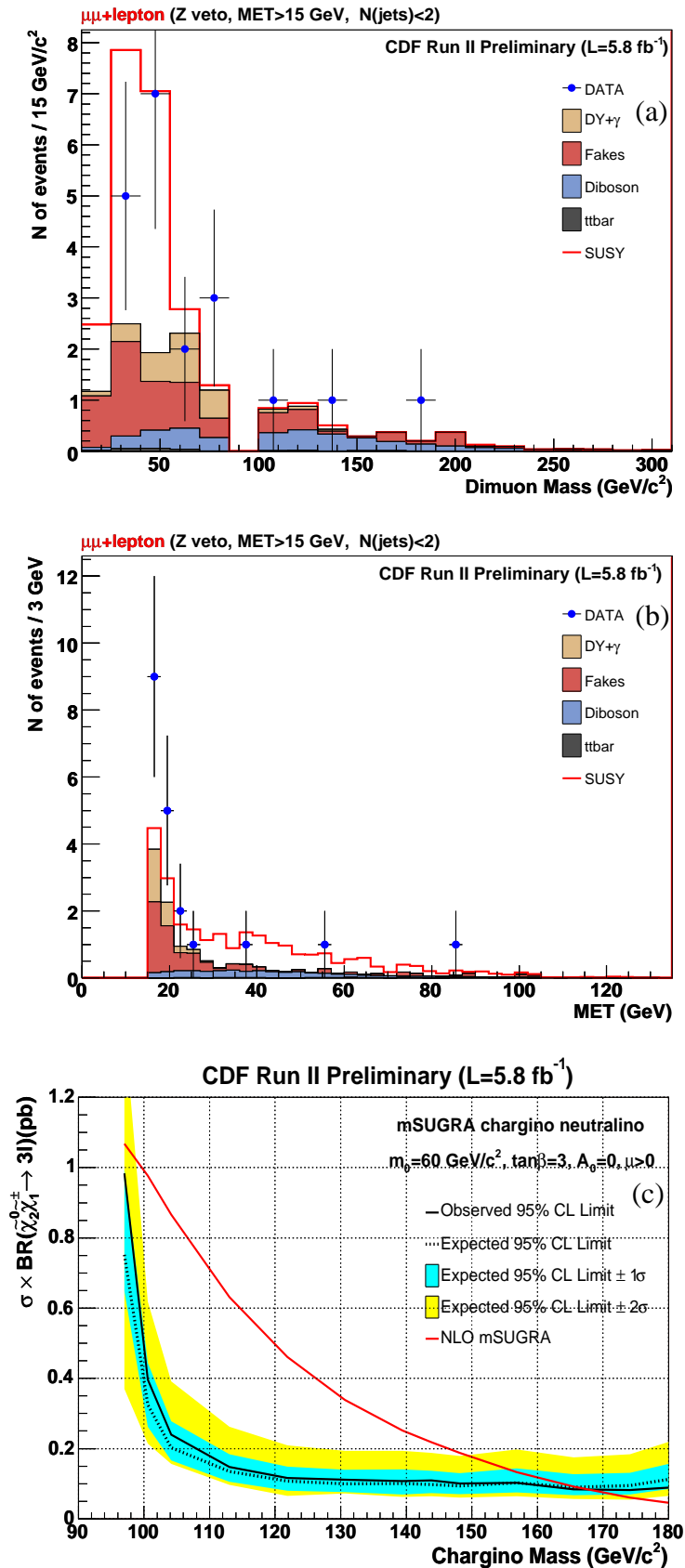


Figure 12. CDF tri-lepton searches [23]. (a) The summed missing p_T and E_T in the $e\tau$ channel; (b) The tau cluster, E_T , in the $\mu\tau$ channel.

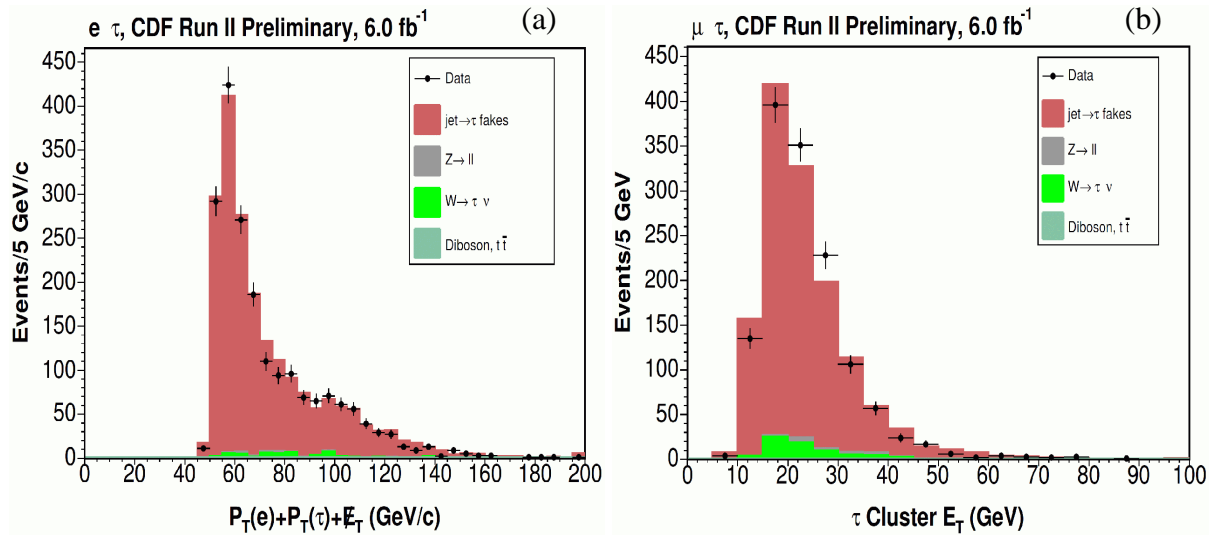
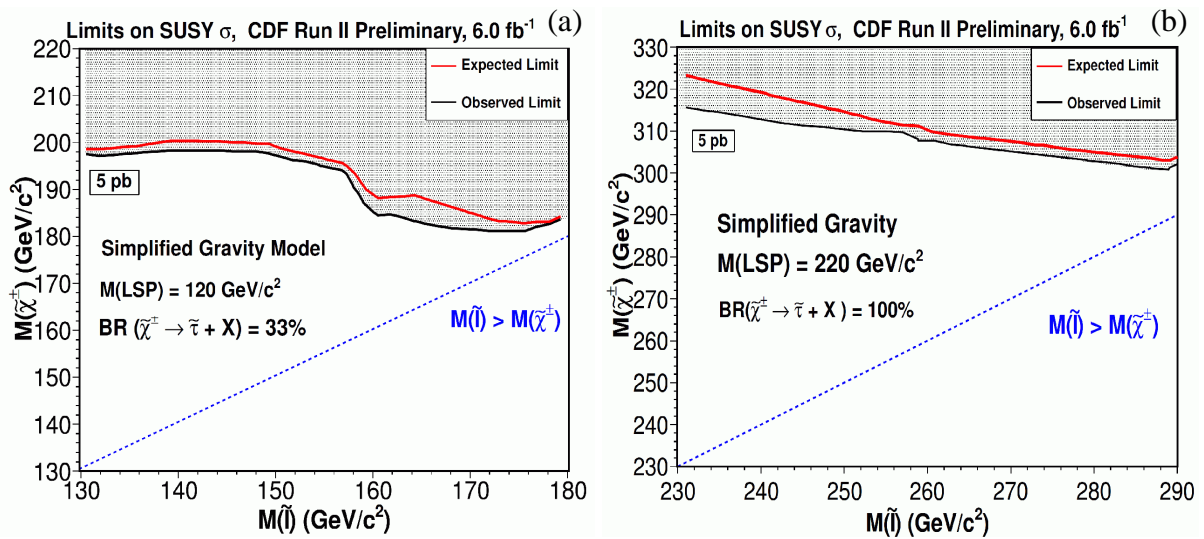


Figure 13. CDF tri-lepton searches in the $\ell\tau$ channel. The limits are at a 95% CL for a simplified gravity model with a 33% and 100% decay branching of charginos into scalar taus [23]. (a) for a 120 GeV lightest supersymmetric particle (LSP); (b) for a 220 GeV LSP.



2.3. Gluinos and Scalar Quarks

Depending on the masses of squarks and gluinos, either $\tilde{q}\tilde{q}^*$, $\tilde{g}\tilde{g}$ or $\tilde{q}\tilde{g}$ could be produced. For gluinos heavier than squarks, squark pair-production dominates, leading to a signature of two acoplanar jets and missing energy from the escaping neutralino. If the squarks are heavier than the gluinos, gluino pair-production is expected, leading to four or more jets. If both masses are about equal, squark-gluino production is expected. Figure 14 [25] shows a summary of the production cross-sections for different reactions involving supersymmetric particles. The mass range for a cross-section of about 1 pb is largest for scalar quark pair-production. The figure also shows the mass limits from early results with

0.3 fb^{-1} [3,4] and sensitivity expectations for two, four and 8 fb^{-1} luminosity per experiment [19].

These expectations are compared to the results from analyses with higher data statistics. Results from $D\bar{D}$ with 2.1 fb^{-1} are shown in Figures 15–17 [26], and results from CDF with 2.0 fb^{-1} are shown in Figures 18 and 19 [27]. For both experiments, the achieved sensitivity for gluino masses is about 300 GeV at 95% CL for large squark masses. This is consistent with the expectations from 2005 (Figure 14b [19]). No indication of a signal is observed, and limits are set in the $(m_{\tilde{g}}, m_{\tilde{q}})$ and $(m_0, m_{1/2})$ planes.

Figure 14. (a) The Next-to-Leading-Order (NLO) production cross-sections included in PROSPINO (PROduction of Supersymmetric Particles In Next-to-leading Order) as a function of the final state particle mass. The arrows indicate the SUGRA inspired scenario: $m_{1/2} = 150 \text{ GeV}$, $m_0 = 100 \text{ GeV}$, $A_0 = 300 \text{ GeV}$, $\tan\beta = 4$, $\mu > 0$. All cross-sections are given at the average mass scale of the massive final-state particles [25]; (b) $D\bar{D}$ squark-gluino searches. Excluded regions at 95% CL in the gluino and squark mass plane by direct searches interpreted in the mSUGRA framework with $\tan\beta = 3$, $A_0 = 0$, $\mu < 0$. The region excluded by this analysis and previous $D\bar{D}$ Run-II results [3,4] in the most conservative hypothesis (σ_{\min}) is shown in dark shading. The thick (dotted) line is the limit of the observed (expected) excluded region. The band delimited by the two dashed lines shows the effect of the Parton Distribution Function (PDF) choice and of the variation of renormalization and factorization scale by a factor of two. Regions excluded by previous experiments are indicated in light shading [28–34]. The two thin lines indicate the indirect limits inferred from the LEP2 chargino and slepton searches [35]. The region where no mSUGRA solution can be found is shown as hatched. With 0.31 fb^{-1} , only a small region beyond the LEP limits near the diagonal was excluded. The sensitivity reach with larger luminosities is also shown [19].

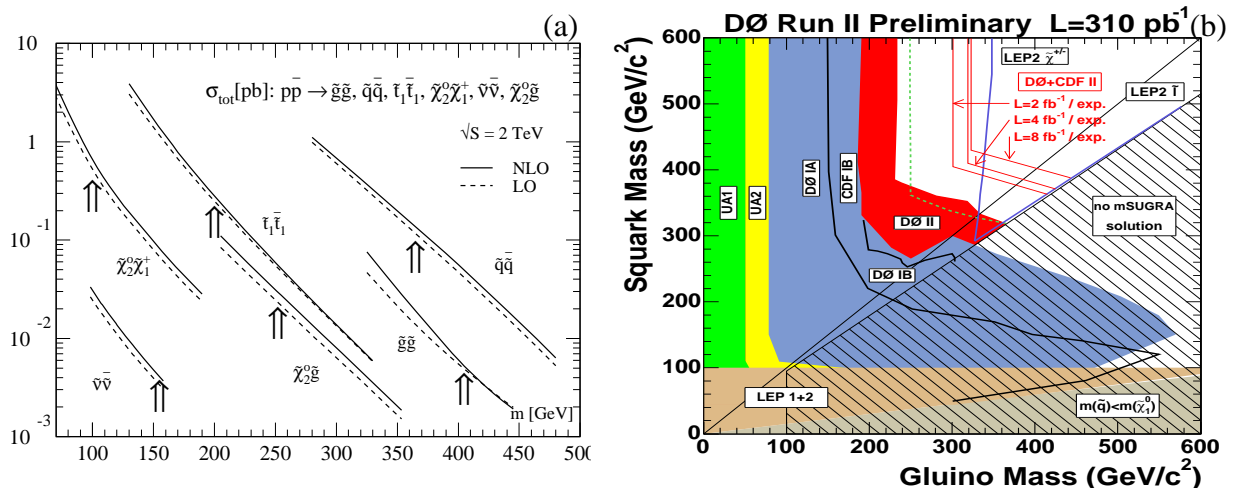


Figure 15. $D\bar{D}$ squark-gluino searches, copyright (2008), with permission from Elsevier [26]. Distributions of \cancel{E}_T after applying all analysis criteria except the one on \cancel{E}_T for the “di-jet” (a); “three-jets” (b); and “gluino” (c) analyses. The signal drawn corresponds to $(m_0, m_{1/2}) = (25, 175)$ GeV, $m_{\bar{q}} = m_{\bar{g}} = 410$ GeV and $(m_0, m_{1/2}) = (500, 110)$ GeV from left to right. The fitted Quantum ChromoDynamics (QCD) background contribution is also shown.

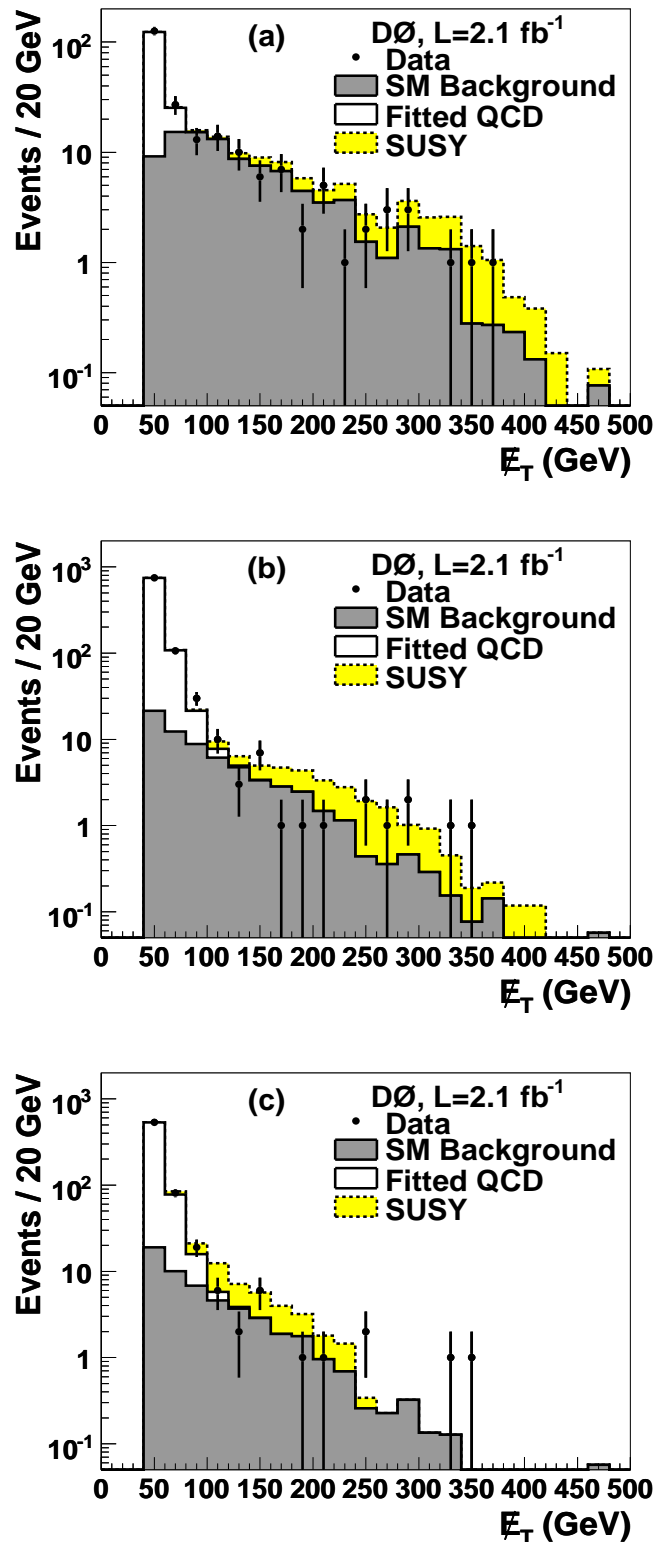


Figure 16. DØ squark-gluino searches, copyright (2008), with permission from Elsevier [26]. Upper limits at 95% CL on squark-gluino production cross-sections are shown for $\tan\beta = 3$, $A_0 = 0$, $\mu < 0$, observed (closed circles) and expected (opened triangles), combining the analyses for $m_0 = 25$ GeV (a); $m_{\tilde{q}} = m_{\tilde{g}}$ (b); and $m_0 = 500$ GeV (c). The nominal production cross-sections are also shown. The shaded bands correspond to the uncertainties from the PDF, and renormalization and factorization scale uncertainties.

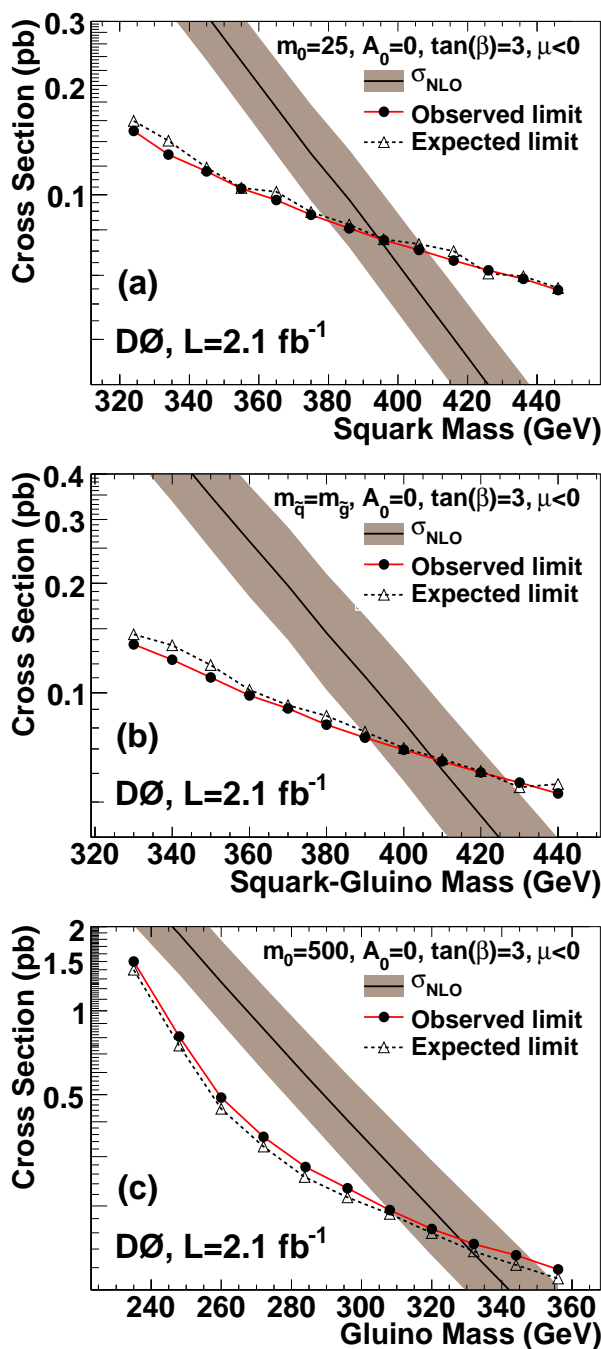


Figure 17. DØ squark-gluino searches, copyright (2008), with permission from Elsevier [26]. (a) Excluded regions at 95% CL in the gluino and squark mass plane by direct searches interpreted in the mSUGRA framework with the same mSUGRA model parameters, as in Figure 14, for 2.1 fb^{-1} data; (b) Region excluded at the 95% CL in the $(m_0, m_{1/2})$ plane for the mSUGRA framework with $\tan\beta = 3$, $A_0 = 0$, $\mu < 0$ (dark shaded area). The thick line is the limit of the excluded region for the σ_{\min} hypothesis. The corresponding expected limit is the dashed line. The band delimited by the two dotted lines shows the effect of the PDF choice and of the variation of renormalization and factorization scale by a factor of two. Regions excluded by the LEP2 chargino and slepton searches are indicated in light shading [35]. The region where there is no electroweak symmetry breaking is shown in black.

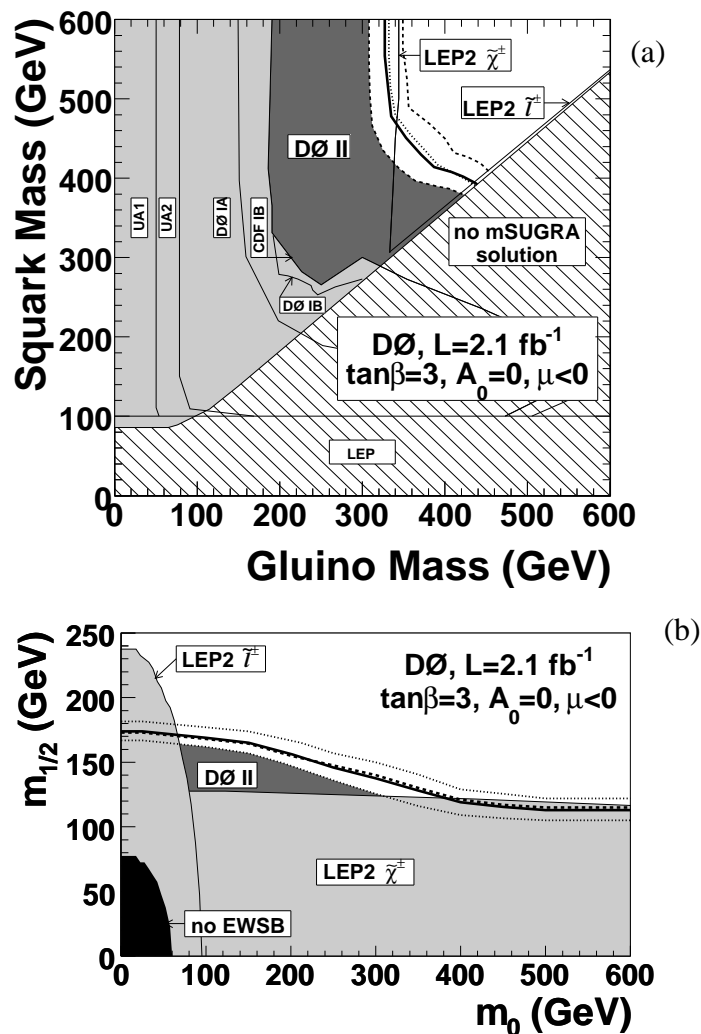


Figure 18. CDF squark-gluino searches, copyright (2009), with permission by the American Physical Society [27]. **(a)** Measured H_T and \cancel{E}_T distributions (black dots) in events with at least two (**bottom**), three (**middle**), and four (**top**) jets in the final state compared to the Standard Model (SM) predictions (solid lines) and the SM + mSUGRA predictions (dashed lines). The shaded bands show the total systematic uncertainty in the SM predictions; **(b)** The observed (solid lines) and expected (dashed lines) 95% CL upper limits on the inclusive squark and gluino production cross-sections as a function of $m_{\tilde{q}}$ (**left**) and $m_{\tilde{g}}$ (**right**) in different squark and gluino mass relations, compared to NLO mSUGRA predictions (dashed-dotted lines). The shaded bands denote the total uncertainty in the theory.

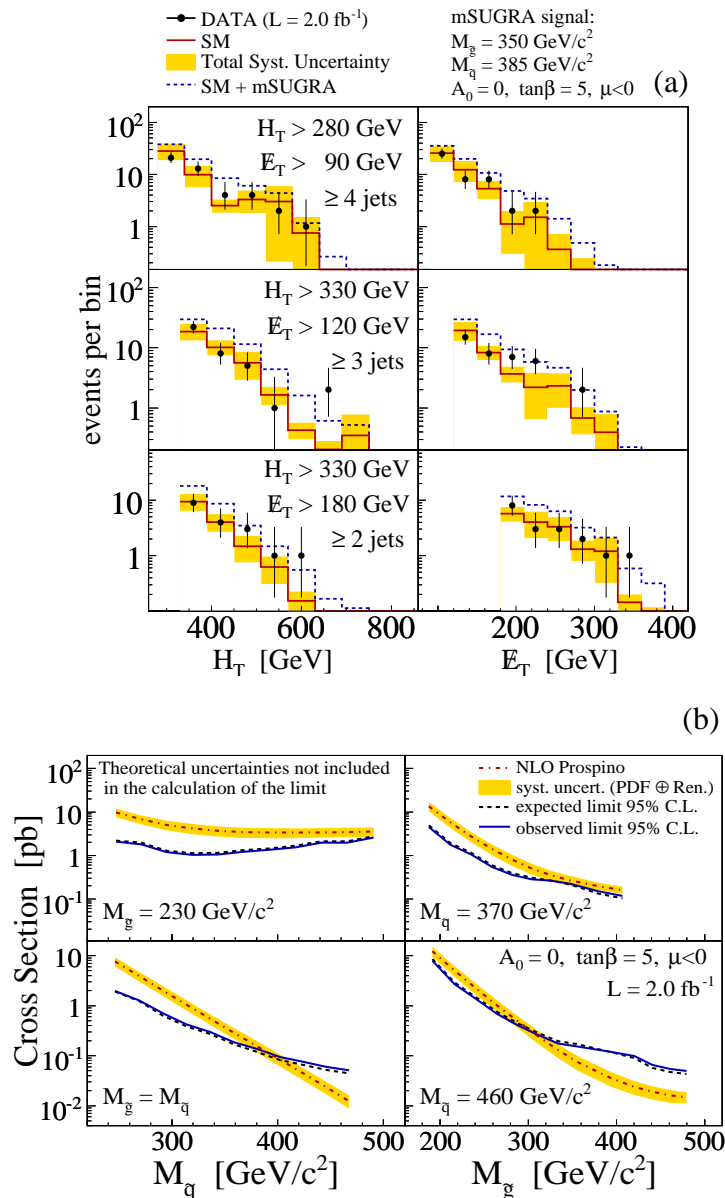
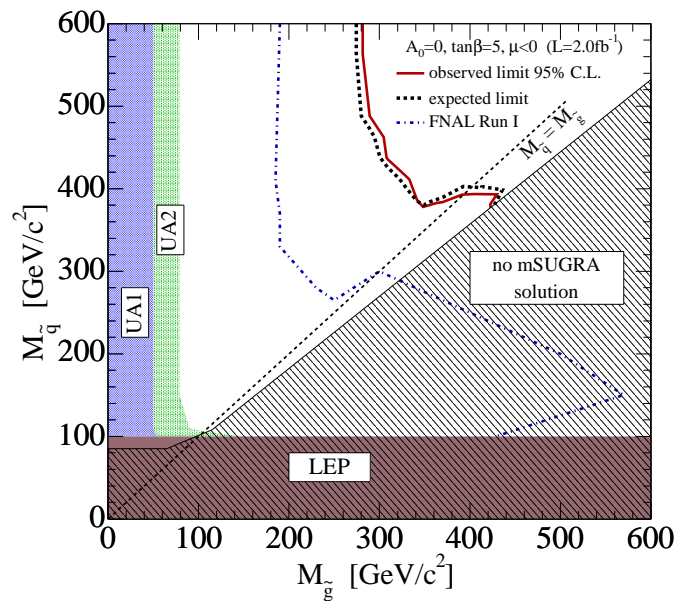


Figure 19. CDF squark-gluino searches, copyright (2009), with permission by the American Physical Society [27]. The exclusion plane at 95% CL as a function of squark and gluino masses in an mSUGRA scenario with $A_0 = 0$, $\mu < 0$ and $\tan\beta = 5$. The observed (solid line) and expected (dashed line) upper limits are compared to previous results from SPS and LEP experiments at CERN (shaded bands), and from the Run-I at the Tevatron (dashed-dotted line) [28–34]. Unlike in Figure 17 where the LEP2 chargino and slepton search results are shown for the given mSUGRA model point, here, only the limits from LEP squark searches are presented. The hatched area indicates the region in the plane with no mSUGRA solution.



2.4. Scalar Tops

Scalar top quarks (stops) decay almost instantly. The most important decay modes in the Tevatron kinematic reach are illustrated in Figure 20. The signature of pair-production of light scalar top quarks is characterized by two c-quark jets and missing energy in the $\tilde{\chi}_1^0 c$ decay mode. In 2005 (0.163 fb^{-1} analyzed luminosity), the experimental cross-section sensitivity approached the expected signal cross-section (Figure 21a [36,37]) at a stop mass of about 110 GeV.

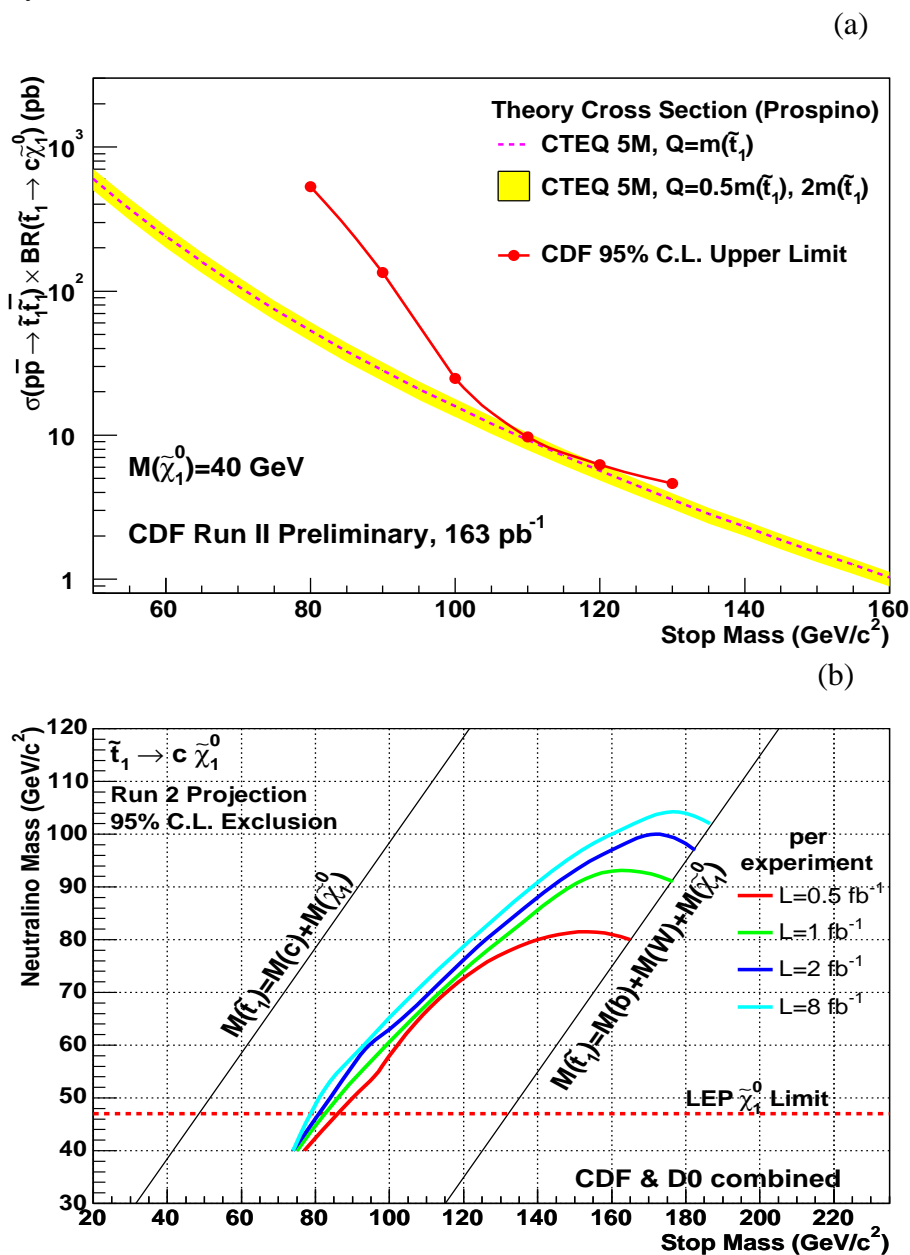
Figure 20. (a) $\tilde{t}_1 \rightarrow \tilde{\chi}_1^0 c$ diagram; (b) $\tilde{t}_1 \rightarrow \tilde{\chi}_1^\pm b \rightarrow b \ell^+ \tilde{\nu}$ diagram.



Higher luminosity was required to reach sensitivity for the scalar top mass of up to about 160 to 180 GeV, as shown in Figure 21b [36,37]. Scalar top results from the DØ collaboration with 1 fb^{-1} for the $\tilde{\chi}_1^0 c$ mode are shown in Figure 22 [38]. Results from the CDF collaboration with 2.6 fb^{-1} , including the development of the excluded stop-neutralino mass region, are shown in Figures 23 and 24 [39].

As seen in Figure 24b, a minimum stop-neutralino mass difference of at least about 35 GeV is required for sensitivity at 95% CL. This is in contrast to e^+e^- colliders, like the LEP [6] or the International Linear Collider (ILC) [40,41], which have also sensitivity for small mass differences.

Figure 21. (a) CDF scalar top cross-section limit at 95% CL [36]; (b) CDF and DØ scalar top sensitivity reach [37].



(a)

(b)

Figure 22. $D\bar{D}$ scalar top searches in the $\tilde{\chi}_1^0 c$ mode, copyright (2008), with permission from Elsevier [38]. (a) Distributions of H_T for a signal with $m_{\tilde{t}} = 150$ GeV and $m_{\tilde{\chi}_1^0} = 70$ GeV (hatched histogram); (b) The final distributions of \cancel{E}_T for the data (points with error bars), SM background (histogram) and a signal with $m_{\tilde{t}} = 150$ GeV and $m_{\tilde{\chi}_1^0} = 70$ GeV (hatched histogram).

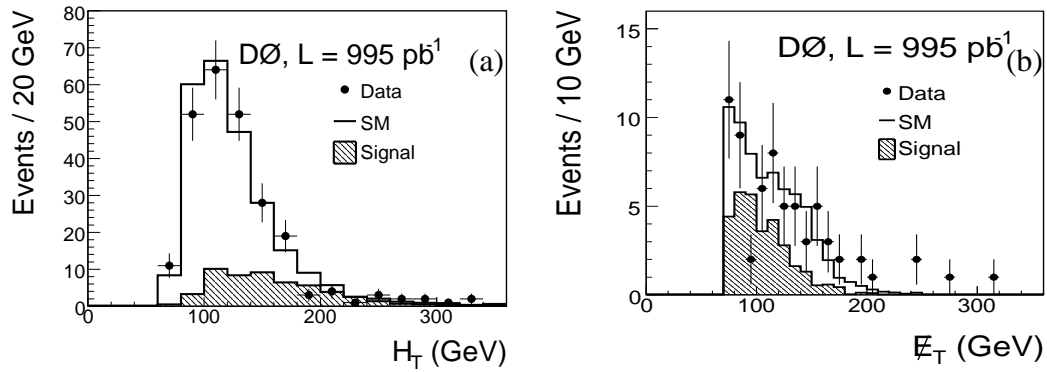


Figure 23. CDF scalar top searches [39]. (a) Neural network output to reject the heavy flavor (HF) QCD background. The arrow indicates the applied selection cut; (b) Neural network output for the final discriminant used to extract the limits.

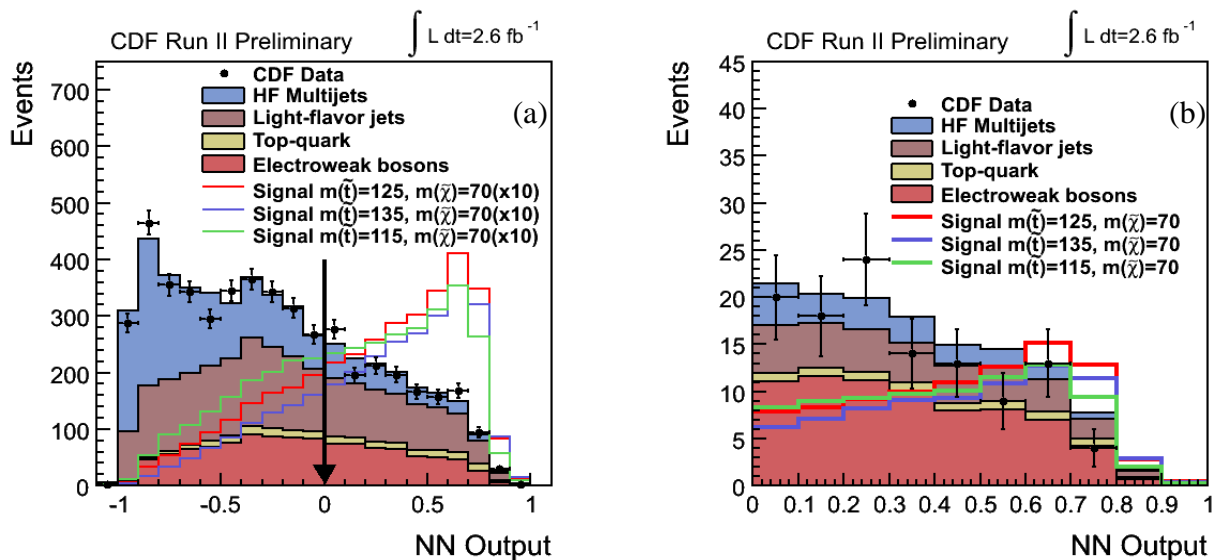
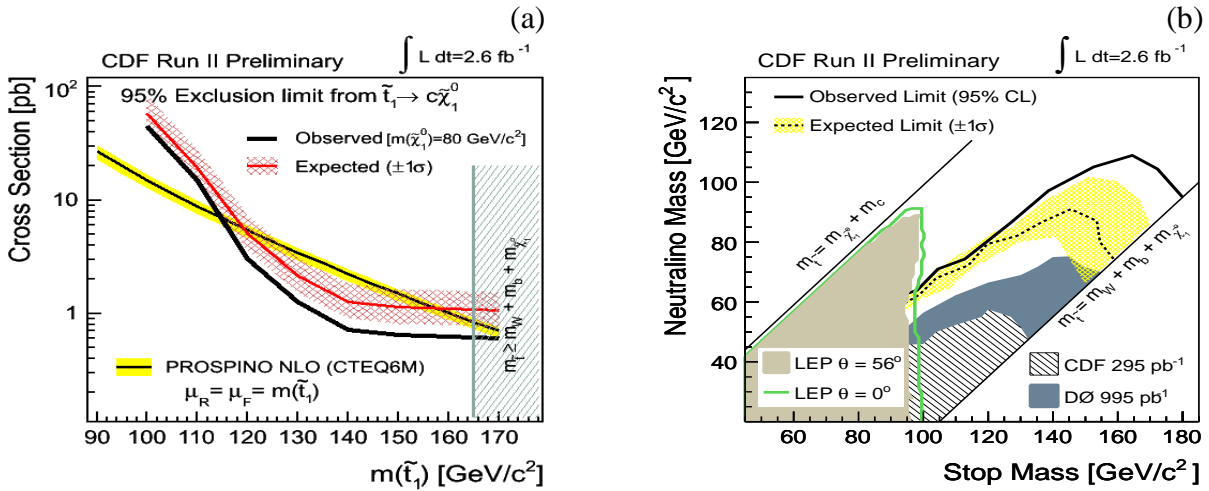


Figure 24. CDF scalar top searches [39]. (a) The observed (black line) and expected (red line) cross-section limits at 95% CL assuming a 80 GeV neutralino with 1σ uncertainty bands. The expected cross-section in NLO calculation is also shown; (b) The excluded region at 95% CL in the scalar top mass *versus* the neutralino mass plane. Regions excluded by previous analyses [42–44] are also shown.



In the first part of this section, the $\tilde{\chi}_1^0 c$ mode was addressed. In the following, the mode $\tilde{\chi}_1^\pm b$ is reviewed. An early DØ search for the $\tilde{t}_1\tilde{t}_1 \rightarrow b\bar{b}\mu^+\mu^-\tilde{\nu}\tilde{\nu}$ reaction was performed with 0.339 fb⁻¹ data, and the results are shown in Figure 25 [45]. Updated DØ results for the search in the electron plus muon and di-electron final states were released by the DØ collaboration for 1.0 fb⁻¹ data [46]. CDF scalar top quark search results with 1.0 fb⁻¹ for the ee, eμ and μμ channels are shown in Figures 26 and 27 [47] for the $\tilde{\chi}_1^\pm b$ mode. Recent results from DØ with 5.4 fb⁻¹ are shown in Figures 28 and 29 [48] for the eμ final state.

Figure 25. DØ $\tilde{t}_1\tilde{t}_1 \rightarrow b\bar{b}\mu^+\mu^-\tilde{\nu}\tilde{\nu}$ searches [45]. (a) Di-muon invariant mass; (b) The excluded region at 95% CL in the scalar top *versus* scalar neutrino mass plane.

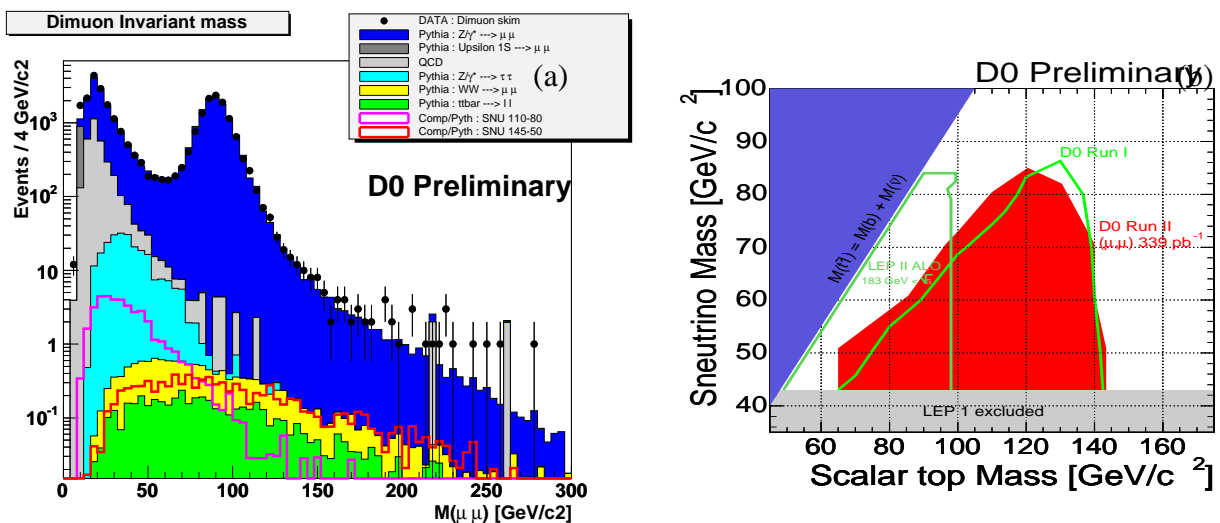


Figure 26. CDF scalar top searches, copyright (2010), with permission by the American Physical Society [47]. Combined ee , $\mu\mu$ and $e\mu$ channels in the scalar top search. The data is shown as the points with error bars (statistical). Shown as stacked histograms are the backgrounds arising from misidentified hadrons and decays-in-flight (ℓ +fake), $b\bar{b}$ and $c\bar{c}$ (HF), Drell–Yan, di-bosons and $t\bar{t}$ production. For reference, the expected signal for $(m_{\tilde{t}}, m_{\tilde{\nu}}) = (150, 75)$ GeV, multiplied by five, is shown as the dashed line. (a) E_T ; (b) H_T .

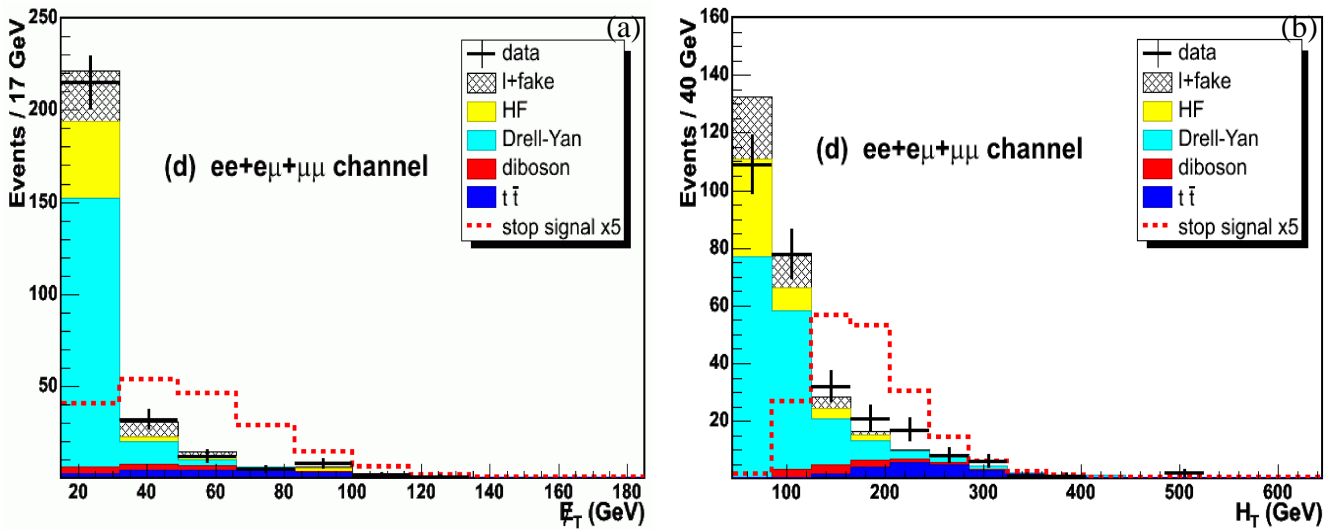


Figure 27. CDF scalar top searches, copyright (2010), with permission by the American Physical Society [47]. (a) The upper limits at 95% CL on the scalar top production cross-section for fixed stop-sneutrino mass differences. The expected cross-section is shown as the solid curve. The band represents the theoretical uncertainty in the cross-section, due to uncertainties in the renormalization and factorization scales and the PDFs; (b) The observed and expected limits in the stop-sneutrino mass plane. The LEP limits are for a mixing angle of zero, which provides the largest reach.

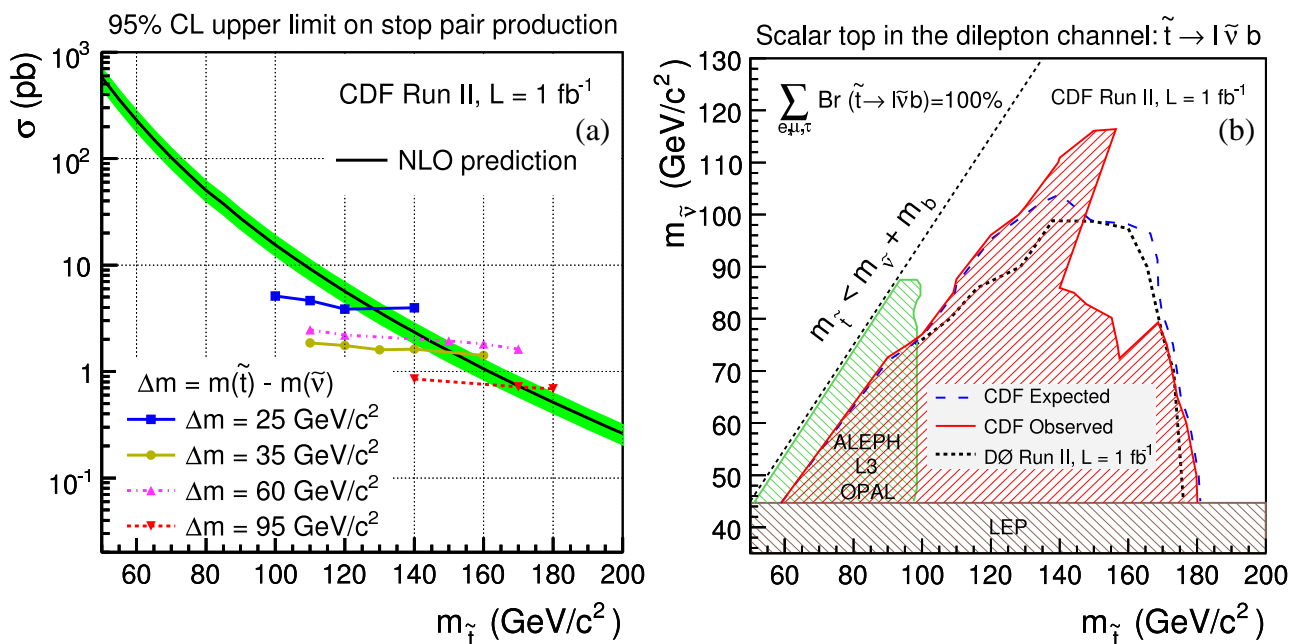


Figure 28. DØ scalar top $\tilde{t}_1\tilde{t}_1 \rightarrow b\bar{b}\mu^+\mu^-\tilde{\nu}\tilde{\nu}$ searches, copyright (2011), with permission from Elsevier [48]. Distributions of E_T (a); Electron p_T (b); And muon p_T (c); Comparing data and all background processes. The thick dashed and thick solid lines represent the small- Δm ($m_{\tilde{t}_1}, m_{\tilde{\nu}}$) = (110,90) GeV, and large- Δm ($m_{\tilde{t}_1}, m_{\tilde{\nu}}$) = (200,100) GeV signal benchmarks, respectively.

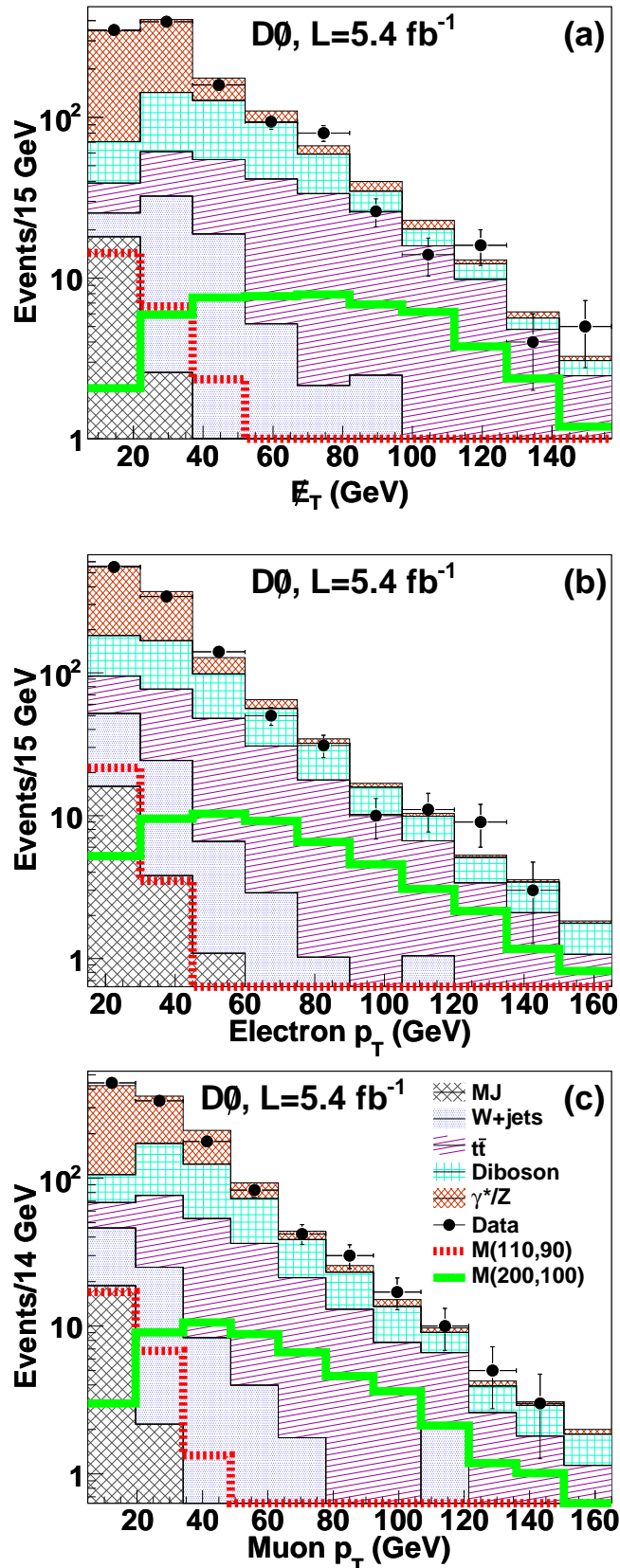
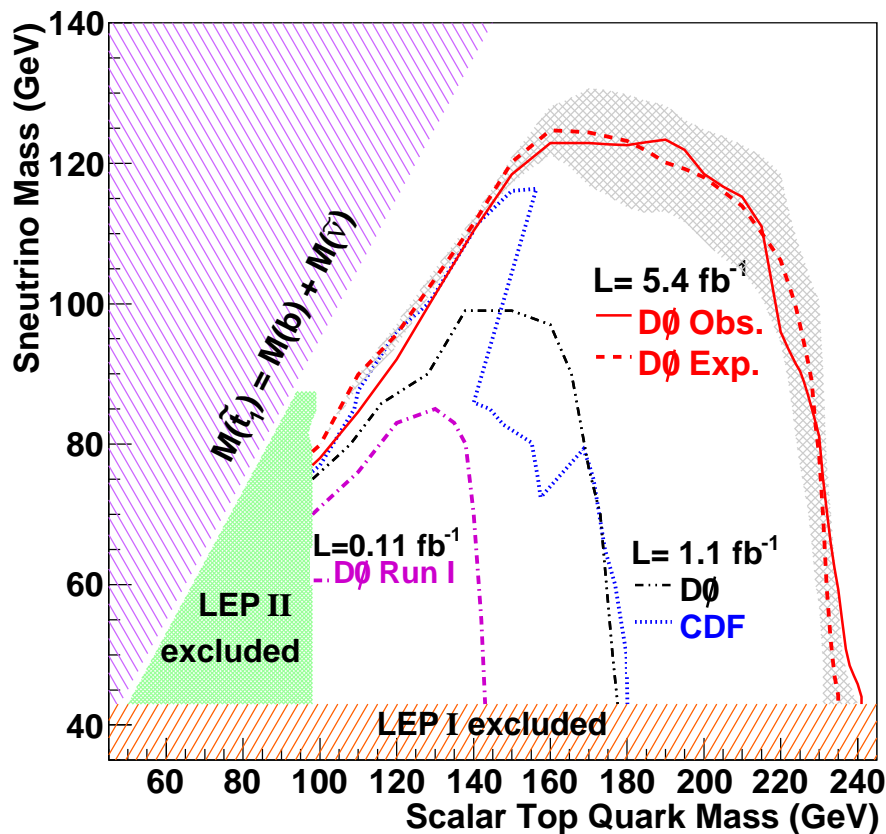


Figure 29. $D\bar{D}$ scalar top $\tilde{t}_1\tilde{t}_1 \rightarrow b\bar{b}\mu^+\mu^-\tilde{\nu}\tilde{\nu}$ searches, copyright (2011), with permission from Elsevier [48]. The observed (expected) 95% CL exclusion region is shown below the solid (dashed) line. The shaded band around the expected limit shows the effects of the scalar top quark pair production cross-section uncertainty. The kinematically forbidden region is represented in the upper left part of the plot. The regions excluded by LEP I and LEP II [6], by previous $D\bar{D}$ searches [46,50] and by a previous CDF search [47] are also shown.



The $D\bar{D}$ collaboration searched for reactions involving τ leptons ($\tilde{t}_1\tilde{t}_1 \rightarrow b\bar{b}\mu\tau\tilde{\nu}\tilde{\nu}$ and $\tilde{t}_1\tilde{t}_1 \rightarrow b\bar{b}\tau\tau\tilde{\nu}\tilde{\nu}$) using 7.3 fb^{-1} . Three neural networks are trained to identify tau decays corresponding to $\tau^\pm \rightarrow \pi^\pm\nu$ (τ_1), $\tau^\pm \rightarrow \pi^\pm\pi^0\nu$ (τ_2), and $\tau^\pm \rightarrow \pi^\pm\pi^\pm\pi^\mp(\pi^0)\nu$ (τ_3). Two signal points are chosen $[m_{\tilde{t}_1}, m_{\tilde{\nu}}] = (180, 60) \text{ GeV}$ and $(120, 80) \text{ GeV}$, labeled “Signal A” and “Signal B” in the following, to illustrate the impact of the selection criteria for large $m_{\tilde{t}_1}$ and Δm (Signal A) and for low $m_{\tilde{t}_1}$ and Δm (Signal B). The selection results are shown in Figure 30 for the higgsino scenario. Limits are shown in Figure 31 for the wino and higgsino scenarios [49].

Figure 30. $D\emptyset$ scalar top searches, copyright (2012), with permission from Elsevier [49]. Distributions of the Boosted Decision Trees (BDT) output discriminants in the higgsino scenario for the sample with $N(\text{jets}) = 1$, for Signal A (a); for Signal B (b); $N(\text{jets}) = 2$, for Signal A (c); for Signal B (d); $N(\text{jets}) > 2$, for Signal A (e); for Signal B (f); where Signal A and B are defined in the text.

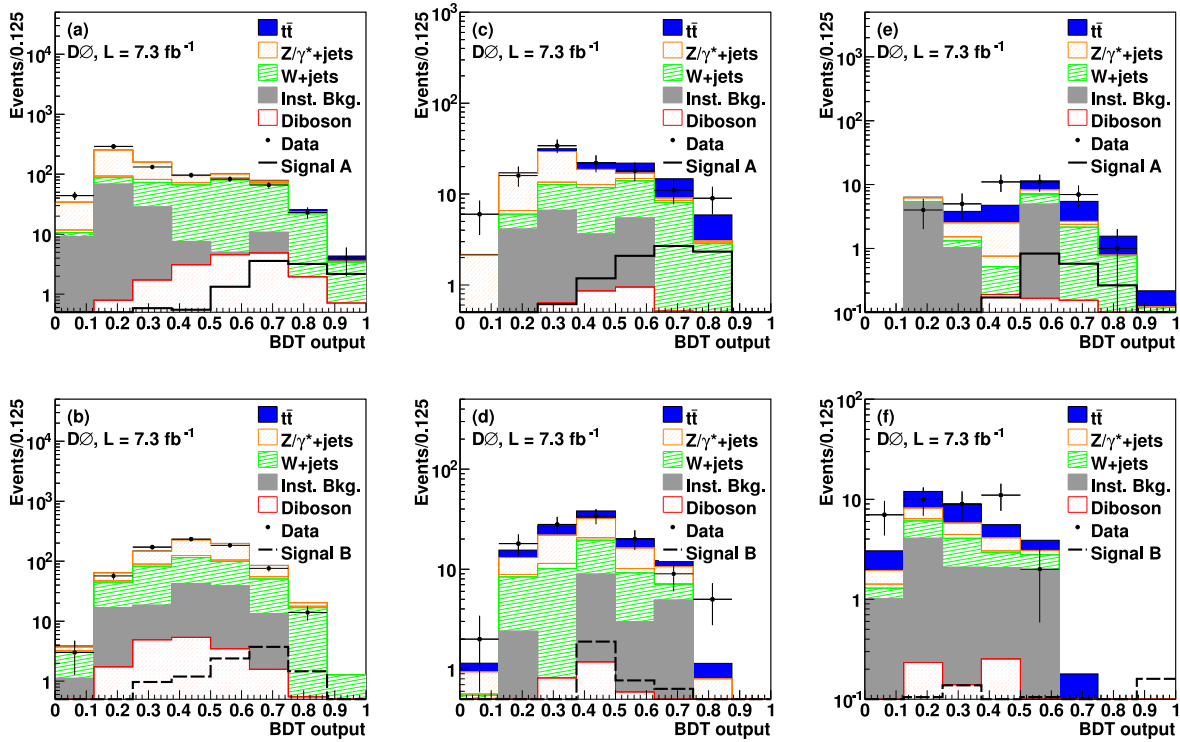
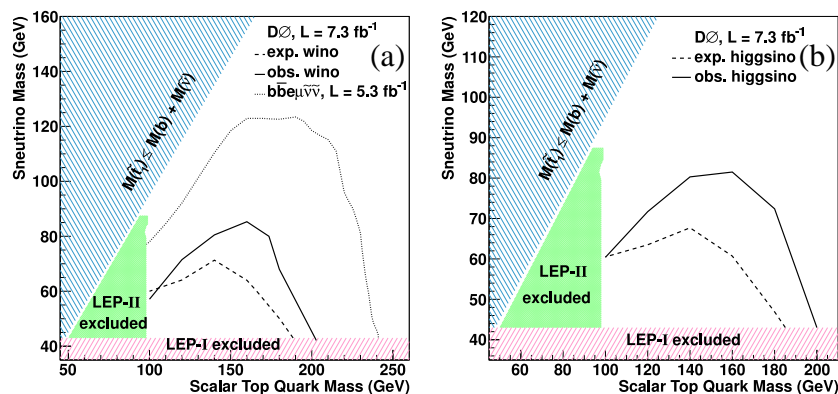


Figure 31. $D\emptyset$ scalar top searches, copyright (2012), with permission from Elsevier [49]. (a) The contour of exclusion at 95% CL in the sneutrino *versus* scalar top quark mass plane obtained for the assumption $B(\tilde{t}_1 \rightarrow b\mu\tilde{\nu}) = B(\tilde{t}_1 \rightarrow b\tau\tilde{\nu}) = 1/3$ (wino scenario). The shaded areas represent the kinematically forbidden region and the LEP-I [51] and LEP-II [6] exclusions. The dashed and continuous lines represent the expected and observed 95% CL exclusion limits. The region excluded by a $D\emptyset$ search [48] for the $\tilde{t}_1\tilde{t}_1 \rightarrow b\bar{b}e\mu\tilde{\nu}\tilde{\nu}$ reaction in the wino scenario is indicated by the dotted line; (b) The contour of exclusion at 95% CL in the sneutrino *versus* scalar top quark mass plane obtained for the assumption $B(\tilde{t}_1 \rightarrow b\mu\tilde{\nu}) = 0.1$ and $B(\tilde{t}_1 \rightarrow b\tau\tilde{\nu}) = 0.8$ (higgsino scenario).



2.5. Scalar Bottoms

In the kinematic reach under investigation, $\tilde{b}_1 \rightarrow \tilde{\chi}_1^0 b$ decays are expected, leading to two b-jets and missing energy in the final state of sbottom pair-production. In order to demonstrate the progress at the Tevatron, first, the early results are shown. The DØ missing E_T and mass limits in the sbottom-neutralino plane are shown in Figure 32 [52,53] for 0.31 fb^{-1} . Recent CDF results with 2.65 fb^{-1} are shown in Figure 33 [54], and results from the DØ collaboration with 5.2 fb^{-1} are shown in Figure 34 [55]. The signal topology of two b-quarks and missing energy is identical to the one from the Higgs boson search $p\bar{p} \rightarrow ZH \rightarrow \nu\bar{\nu}b\bar{b}$ [56–58].

Figure 32. DØ scalar bottom searches, copyright (2006), with permission by the American Physical Society [52,53]. (a) The missing E_T distribution for the 0.31 fb^{-1} data; (b) The sbottom-neutralino mass limits at 95% CL.

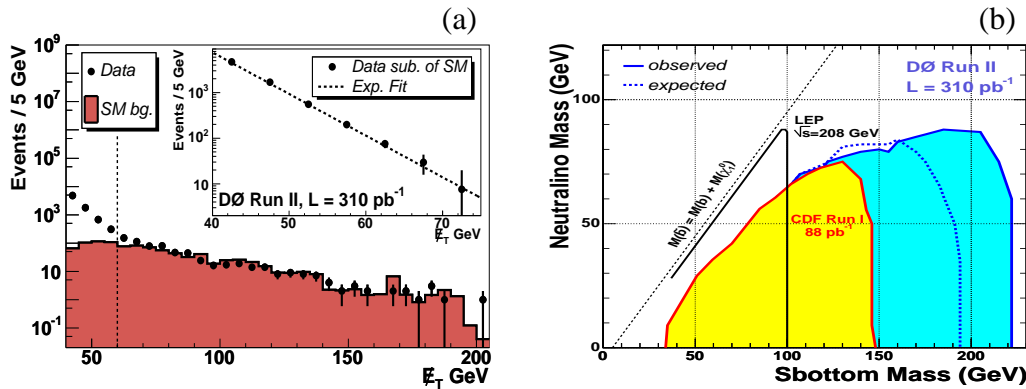


Figure 33. CDF scalar bottom searches, copyright (2010), with permission by the American Physical Society [54]. (a) Measured E_T and $H_T + E_T$ distributions (black dots) for low- Δm (top) and high- Δm analyses (bottom), compared to the SM predictions (solid lines) and the SM + MSSM predictions (dashed lines). The shaded bands show the total systematic uncertainty on the SM predictions; (b) The exclusion plane at 95% CL as a function of sbottom and neutralino masses. The observed and expected upper limits from this analysis are compared to previous results from CDF and DØ experiments at the Tevatron in Run II and from LEP experiments at CERN with squark mixing angle $\theta = 0^\circ$. The hatched area indicates the kinematically prohibited region in the plane.

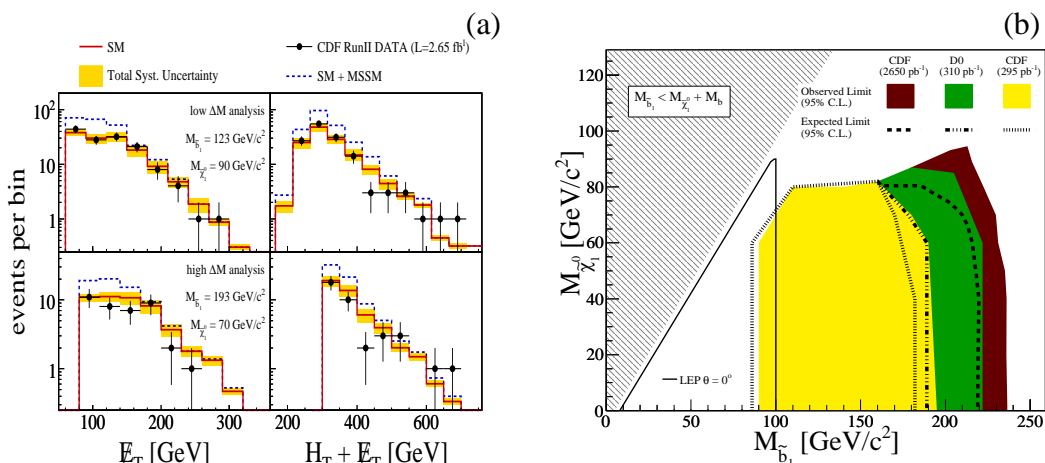
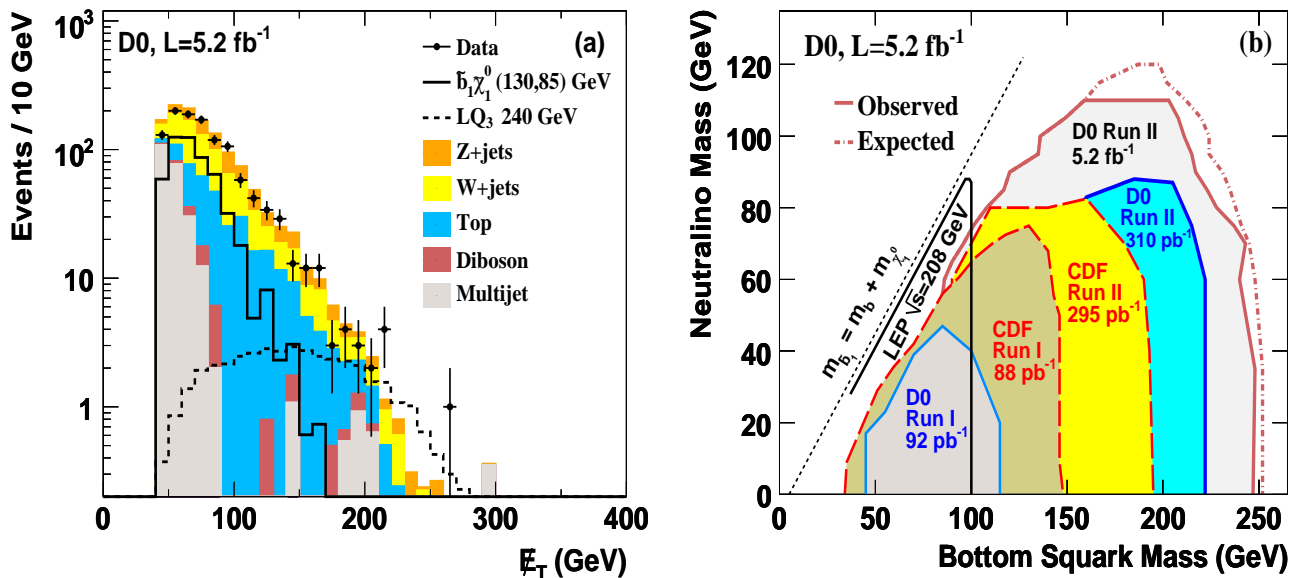


Figure 34. $D\bar{D}$ scalar bottom searches, copyright (2010), with permission from Elsevier [55].
 (a) The missing E_T distribution for 5.2 fb^{-1} data; (b) The sbottom-neutralino mass limits.



The increase of the sensitivity and the extension of the excluded region to higher sbottom masses are illustrated. Note that in Figure 34b for a 100 GeV sbottom mass, sensitivity is achieved for a mass difference $m_{\tilde{b}} - m_{\tilde{\chi}_1^0}$ of about 30 GeV, and for a 150 GeV sbottom for a mass difference of about 50 GeV. In contrast to these large values, the LEP e^+e^- collider achieved sensitivity over the whole kinematic reach for a mass difference close to $m_{\tilde{b}} - m_{\tilde{\chi}_1^0} = m_b$.

2.6. Charged Massive Particles

Many quasi-stable particles could appear in supersymmetric models (In particular, the next to lightest supersymmetric particle can have a long lifetime). Searches for quasi-stable particles were performed and interpretations given in several supersymmetric models. The production of stable scalar tau leptons would result in a signature in the detector similar to a pair of muons, but with mass and speed inconsistent with the production of muons. The speed $\beta = v/c$ of these charged massive particles is expected to be significantly different compared to muons, as shown in Figure 35a [59]. In the nearly mass-degenerate neutralino-chargino scenario, which occurs naturally in the anomaly-mediated symmetry breaking (AMSB) model, limits are shown on the chargino mass (Figure 35b). Figure 35c shows an example in the MSSM when the chargino is higgsino-like.

Recent results from the $D\bar{D}$ collaboration with 5.2 (6.3) fb^{-1} luminosity exclude a pair-produced long-lived gaugino-like chargino below 267 (278) GeV and higgsino-like charginos below 217 (244) GeV at 95% CL [60,61], as well as long-lived scalar top quarks with mass below 285 GeV. These results are shown in Figures 36 and 37.

The scalar top quarks can have a distinct signature, since they appear in charged or neutral stop hadrons. These hadrons may flip their charge as they pass through the detector. In the simulation, approximately 60% of stop hadrons are charged following initial hadronization, *i.e.*, 84% of the events

will have at least one charged stop hadron. Furthermore, scalar top hadrons may flip their charge through nuclear interactions, as they pass through material.

It is assumed that stop hadrons have a probability of 2/3 of being charged after multiple nuclear interactions and anti-stop hadrons, a probability of 1/2 of being charged, consistent with the numbers of possible scalar top and anti-stop hadronic final states. CDF performed a search for long-lived charged massive particles produced in 1.0 fb^{-1} using a high transverse-momentum p_T muon trigger. The search sets an upper bound on the production cross-section. Interpreting this result within the context of a stable scalar top-quark model resulted in a lower limit at 95% CL on the particle mass of 249 GeV, as shown in Figure 38 [62].

Figure 35. $D\bar{D}$ searches for charged massive particles [59]. (a) The speed significance $(1 - \text{speed})/\sigma_{\text{speed}}$ of charged massive particles; (b) The anomaly-mediated symmetry breaking (AMSB) gaugino interpretation; (c) The MSSM higgsino interpretation.

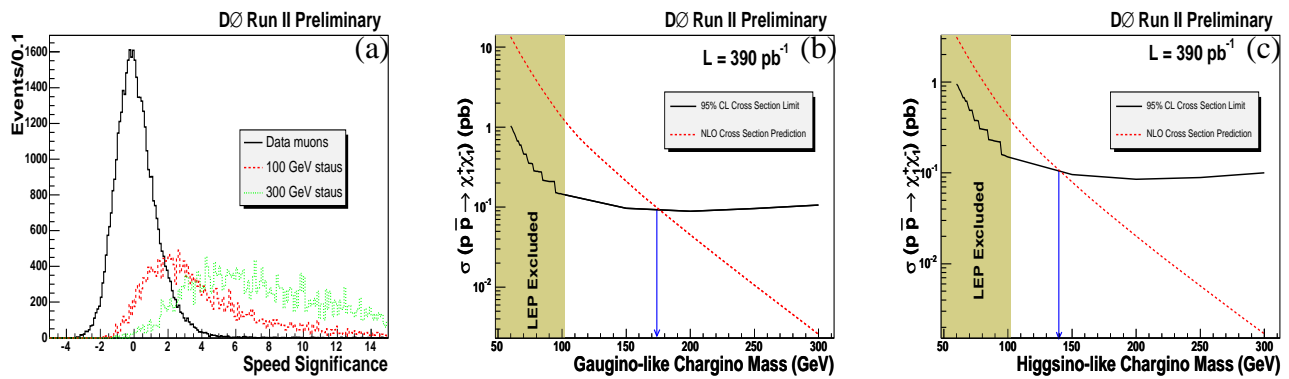


Figure 36. $D\bar{D}$ searches for charged massive particles, copyright (2012), with permission by the American Physical Society [60]. (a) Distributions of speed β ; (b) The distribution of dE/dx for data, background and signal (gaugino-like charginos with a mass of 100 and 300 GeV) that pass the selection criteria. The histograms have been normalized in order to have the same number of events. The scale of the dE/dx measurements is scaled so that the dE/dx of muons from $Z \rightarrow \mu\mu$ events peak at one. All entries exceeding the range of the histogram are added to the last bin.

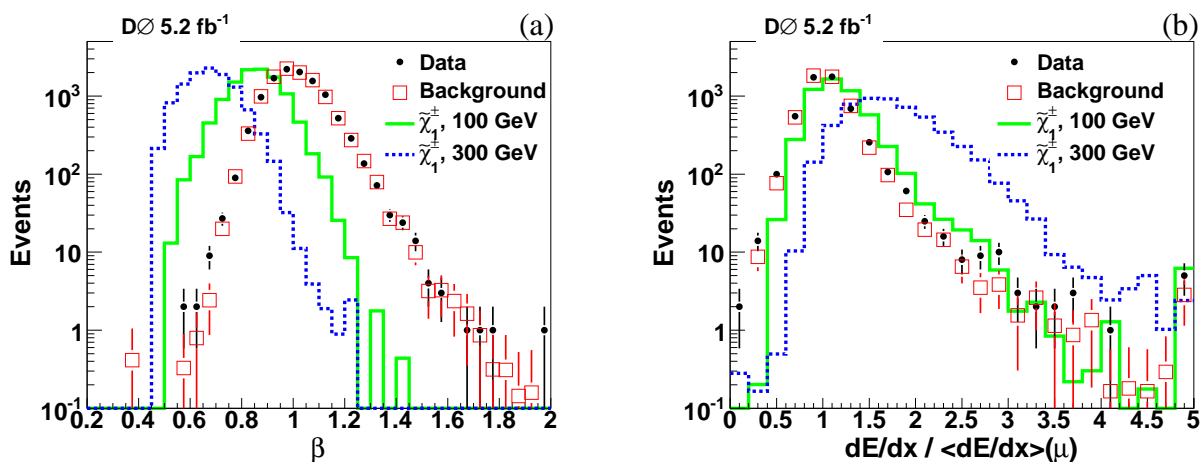


Figure 37. $D\bar{D}$ searches for charged massive particles, copyright (2012, 2013), with permission by the American Physical Society [60,61]. Cross-section limits at 95% CL as a function of mass. (a) Gaugino-like charginos; (b) Higgsino-like charginos; (c) Stop squarks. The stop squark limits are displayed for the assumed charge flipping (38% charge survival probability) and for no charge flipping (84% charge survival probability).

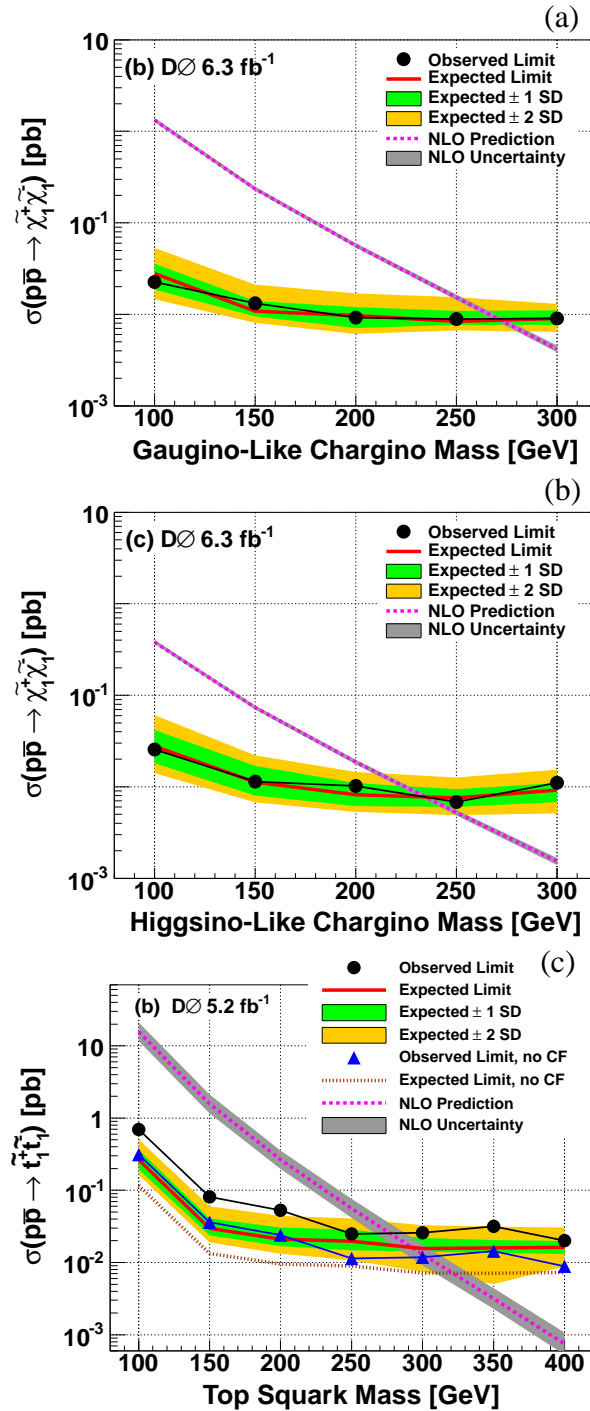
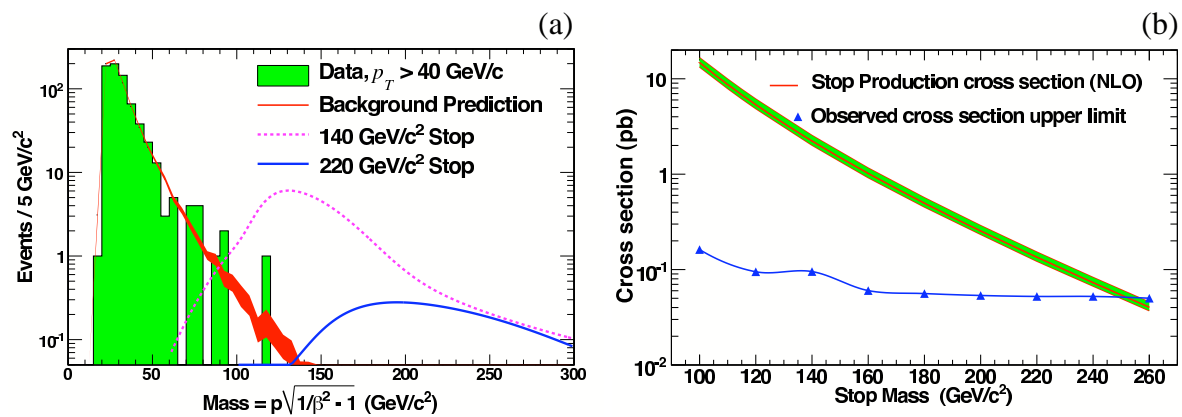


Figure 38. CDF searches for charged massive particles, copyright (2009), with permission by the American Physical Society [62]. (a) Observed (histogram) and predicted (band) mass distributions for candidate tracks in the muon sample. The curves on the right show the simulated distributions expected for a 140 and a 220 GeV long-lived stop; (b) Observed 95% CL limits on the production cross-section of a stable top-squark pair (points), compared to the theoretical NLO cross-section (curve). The band represents theoretical and parton distribution function uncertainties. The intersection of the band with the limit curve yields a lower mass limit for a stable top squark of 249 GeV.

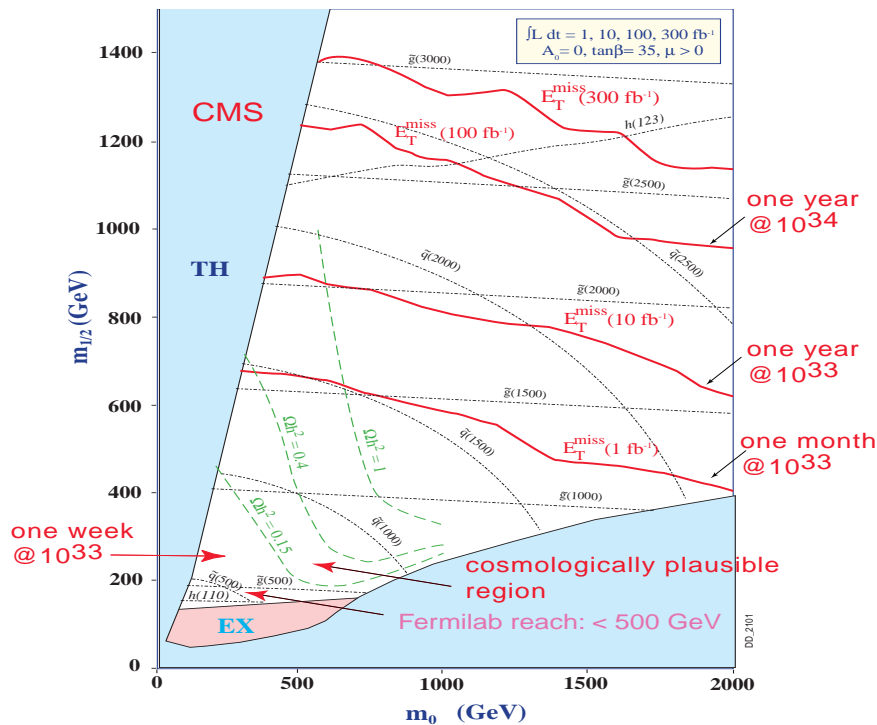


3. LHC

In 2005, it was planned that the LHC would operate up to 14 TeV, which is about seven times the center-of-mass energy of the Tevatron. Sensitivity prospects for discovering supersymmetric particles were given for this LHC operation scenario. In the first stage, the LHC operated at 7 TeV center-of-mass energy in 2011, increasing to 8 TeV in 2012. Although the corresponding production cross-sections are reduced compared to the design center-of-mass energy, the increased LHC energy compared to the Tevatron greatly extends the reach to discover new particles.

In the search for supersymmetric particles, the LHC has great potential at 14 TeV for a discovery within a short period of data-taking. In order to compare the long-term expectations and the actual achieved sensitivities, an example from 2005 of the expectations at 14 TeV to discover supersymmetry is shown in Figure 39 [63], assuming the mSUGRA model. A variety of supersymmetric reactions are in reach of the LHC sensitivity. While a signature from supersymmetry cannot escape detection at the LHC, determining the precise model structure is a very challenging task. Further precision measurements would be possible at a linear collider, as reviewed, for example, in [64,65]. It will be particular difficult for the LHC to determine the relevant scalar top parameters in the cosmologically interesting region of stop-neutralino co-annihilation, where a future linear collider can perform more precise measurements [40,41].

Figure 39. Squark-gluino 5σ discovery reach for a signal with jets plus missing energy in the mSUGRA model [63]. In the forbidden region on the left (small m_0) the neutralino is not the LSP, and in the lower region (small $m_{1/2}$), there is no electroweak symmetry breaking. The cosmologically plausible region (co-annihilation) is close to the forbidden regions on the left bottom. This cosmological plausible region could be covered within the first period of LHC data-taking at 14 TeV. With the luminosity of 100 fb^{-1} , scalar quarks of up to 2500 GeV could be discovered.



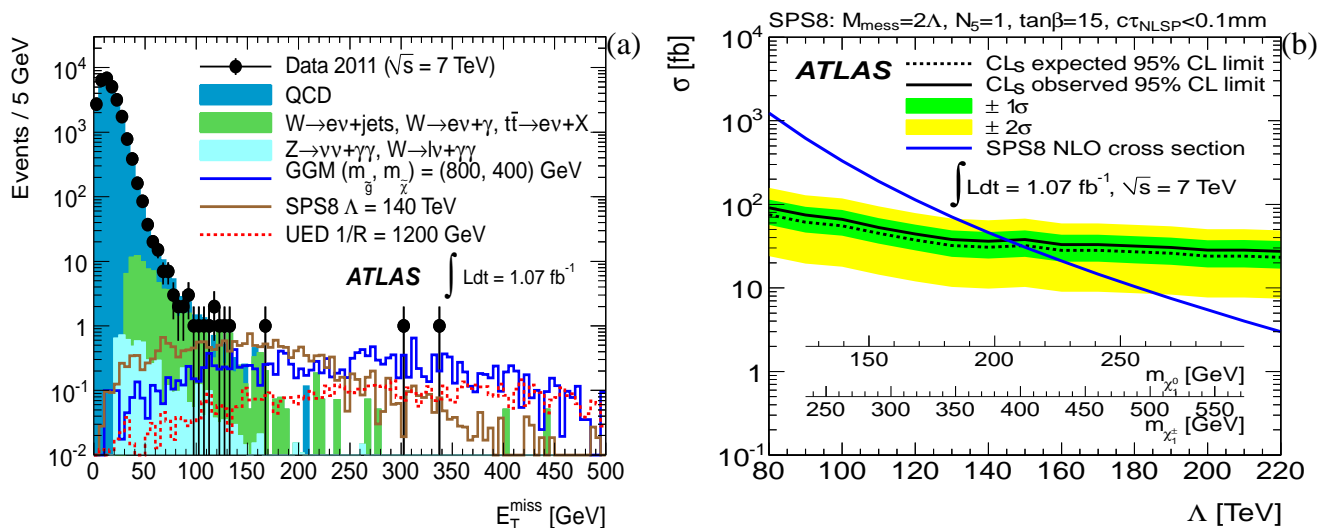
The first LHC results allow, in some cases, a direct comparison with the Tevatron results. Two examples of LHC search results are used for this comparison, first, searches with di-photons and, second, searches for scalar quarks.

As reviewed for the Tevatron (Section 2.1), the LHC results (ATLAS (A Toroidal LHC Apparatus) [66]) are also presented for a specific scenario in the framework of the supersymmetric model, the SPS8 benchmark for gauge-mediated supersymmetry breaking. Similar results were obtained by CMS (Compact Muon Solenoid) [67]. Table 1 compares the limits on the excluded effective Supersymmetry breaking scale, the lightest neutralino mass and the lightest chargino mass between the $D\bar{D}$ results (6.3 fb^{-1} data taken at 1.96 TeV) and the ATLAS results (1.07 fb^{-1} data taken at 7 TeV). It is interesting to note that the LHC superseded the limits with about 1/6 of the luminosity collected at the Tevatron. Figures 5 and 40 show the missing E_T distributions, as well as the SPS8 limits for the Tevatron ($D\bar{D}$) and LHC (ATLAS), respectively.

Table 1. Di-photon results for the SPS8 benchmark from the Tevatron (DØ with 6.3 fb^{-1} data taken at 1.96 TeV) and the LHC (ATLAS with 1.07 fb^{-1} data taken at 7 TeV). The limits on the effective Supersymmetry breaking scale, Λ , the lightest neutralino mass, $m_{\tilde{\chi}_1^0}$, and the lightest chargino mass, $m_{\tilde{\chi}_1^\pm}$, are given at 95% CL.

Accelerator (Experiment)	Λ (GeV)	$m_{\tilde{\chi}_1^0}$ (GeV)	$m_{\tilde{\chi}_1^\pm}$ (GeV)
Tevatron (DØ)	124	175	330
LHC (ATLAS)	145	205	396

Figure 40. LHC (ATLAS) GMSB di-photon searches, copyright (2012), with permission from Elsevier [66]. (a) The missing E_T ; (b) The limit at 95% CL for the SPS8 benchmark parameter scenario.



In the following, the Tevatron results for squark-gluino searches are compared with recent LHC results. The LHC results are also placed into the context of the 14 TeV sensitivity predictions (Figure 39). The squark-gluino searches presented here rely on the separation of QCD background and supersymmetric signal events with a multi-jet and missing energy characteristic. In order to achieve this, a so-called razor variable is defined by the CMS collaboration, which gives the name to this analysis [68]. For the ATLAS collaboration, the ratio, $E_T/\sqrt{H_T}$, is used for the separation of signal and background, where H_T is the scalar sum of the jet momenta [69]. It is a measure of the significance of the E_T in the event. No indication of a signal was observed. The resulting limits in the $(m_0, m_{1/2})$ plane are shown in Figure 41 in the framework of the mSUGRA model (constrained MSSM, CMSSM). The early result from ATLAS nicely displays the increase in sensitivity compared to the Tevatron results (as given in Figure 17 for DØ with 2.1 fb^{-1} and in Figure 19 for CDF with 2.0 fb^{-1}). Recently, ATLAS and CMS published updated results with about 20 fb^{-1} data, each taken at 8 TeV [70,71]. Thus, the lower Tevatron gluino mass limit increased from about 300 GeV (CDF [27], DØ [26]) to a current LHC mass limit above about 1.1 TeV (ATLAS [70], CMS [71]). The LHC has already largely extended the excluded parameter region of supersymmetric models compared to the Tevatron results. This extension is mostly due to the about 3.5–4.0 times higher center-of-mass energy at the LHC. It is also remarkable that first LHC results

with 4.7 fb^{-1} data taken at 7 TeV (2011 running period) excluded a parameter region quite similar to the sensitivity prediction for 1 fb^{-1} at 14 TeV (Figure 39).

The search for scalar top quarks allows a direct comparison between the Tevatron and the first LHC results. At the Tevatron, a scalar top quark mass was excluded up to about 180 GeV (for example, CDF Figure 24 [39] 2.6 fb^{-1} at 2 TeV), while at the LHC for small mass values of the lightest supersymmetric particle, scalar top quark mass values up to around 650 GeV are excluded (for example, CMS Figure 42 [72] 19.5 fb^{-1} at 8 TeV).

Figure 41. LHC squark-gluino searches. Limits in the $(m_0, m_{1/2})$ plane at 95% CL. (a) CMS razor analysis, copyright (2013), with permission by the American Physical Society [68]; (b) ATLAS multi-jet analysis, copyright (2011), with permission from Springer [69]. Details of the Tevatron results are given in Figure 17 for $D\bar{O}$ with 2.1 fb^{-1} and in Figure 19 for CDF with 2.0 fb^{-1} .

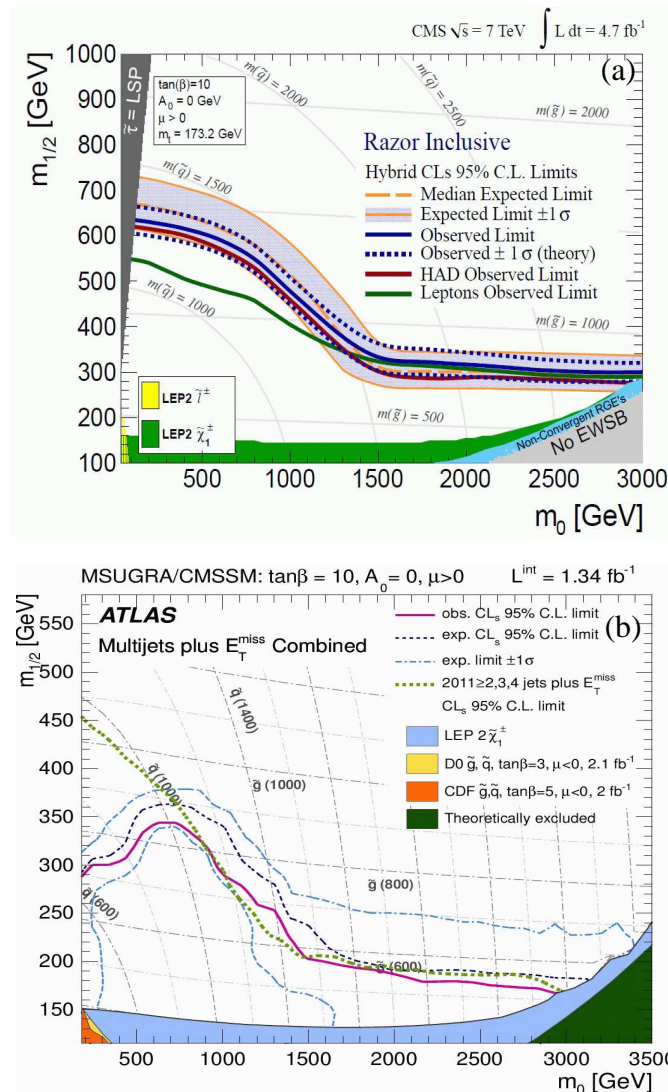
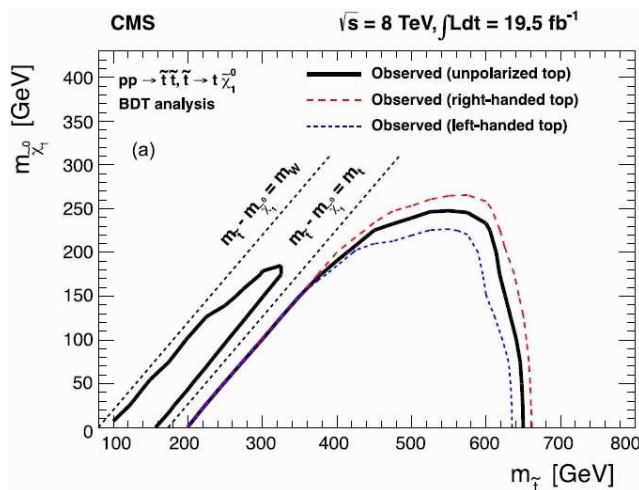


Figure 42. LHC scalar top searches, copyright (2013), with permission from Springer [72]. CMS observed 95% CL excluded regions for the $\tilde{t} \rightarrow \tilde{\chi}_1^0 c$ model for the case of unpolarized, right-handed and left-handed top quarks.



4. Conclusions

The search at the Tevatron for supersymmetric particles was characterized as an era of sensitivity increases compared to the previous results at LEP and a preparation phase for the LHC operation. Results from the Tevatron are reviewed in the context of sensitivity improvements over the last, about, eight years (2005 to 2013). The sensitivity predictions from 2005 agree remarkably well with the achieved results using the full Tevatron dataset. The Tevatron results show impressive progress in sensitivity for supersymmetric signatures involving di-photons, tri-leptons, scalar quarks and gluinos, scalar top and scalar bottom quarks and for charged massive particles. These scientific advances are also based on many new and optimized search techniques and methods, which are directly applicable to current searches at the LHC. The first LHC results based on seven and 8 TeV center-of-mass energies are compared with the 14 TeV LHC predictions from 2005; and they agree well, taking into account the reduced operation energy in the first LHC stage. Examples of Tevatron and initial LHC results have been compared, and the LHC has much extended the sensitivity with respect to the Tevatron results from the 100 GeV scale to the terascale. The achieved experimental Tevatron results show that sensitivities can be reliably predicted for long-term planning of future performances at particle colliders. At the Tevatron, a major step towards discovering supersymmetry or ruling it out was made, and the LHC has taken over this exciting field of research.

Acknowledgments

I would like to thank the colleagues from the LEP, Tevatron and LHC communities for fruitful discussions and for giving suggestions for this review. In particular, I would like to express my thanks to Anna Lipniacka and David Toback for their detailed comments on the manuscript.

Appendix: Overview of Reviewed Analyses

Table A1. Overview of the analyses included in this review.

Search reaction	Experiment	Final state	\mathcal{L} (fb ⁻¹)	Ref. note spring 2005	\mathcal{L} (fb ⁻¹)	Ref. note update
$\tilde{\chi}^+ \tilde{\chi}_2^0$	CDF + DØ	$\gamma\gamma + E_T$	0.202 + 0.263	0504004 [10]		
$\rightarrow \tilde{\chi}_1^0 W^+ \tilde{\chi}_1^0 Z$	DØ	$\gamma\gamma + E_T$			6.3	1008.2133 [11]
$\rightarrow \tilde{G} \gamma W^+ \tilde{G} \gamma Z$	CDF	$\gamma\gamma + E_T$			2.6	0910.3606 [12]
$\tilde{\chi}^+ \tilde{\chi}_2^0$	DØ	$\tau\ell\ell + E_T$	0.325	4740 [15]		
$\rightarrow \tilde{\ell}^+ \nu \tilde{\ell}^+ \ell^-$	DØ	$e\tau\ell + E_T$	0.325	4741 [16]		
$\rightarrow \ell^+ \tilde{\chi}_1^0 \nu \ell^+ \tilde{\chi}_1^0 \ell^-$	DØ	$\mu\tau\ell + E_T$	0.326	4742 [17]		
	DØ	$ee(e\mu)(\mu\mu)(\mu\tau)\ell + E_T$			2.3	0901.0646 [20]
	CDF	$ee(\mu\mu) + E_T$			5.8	10636 [22]
	CDF	$e\tau(\mu\tau) + E_T$			6.0	10611 [23]
$\tilde{q}\tilde{q} \rightarrow q\tilde{\chi}_1^0 q\tilde{\chi}_1^0$	DØ	jets+ E_T	0.31	4737 [3,4]		
$\tilde{q}\tilde{g} \rightarrow q\tilde{\chi}_1^0 q\tilde{q}\tilde{\chi}_1^0$	DØ	jets+ E_T			2.1	0712.3805 [26]
$\tilde{g}\tilde{g} \rightarrow qq\tilde{\chi}_1^0 qq\tilde{\chi}_1^0$	CDF	jets+ E_T			2.0	0811.2512 [27]
$\tilde{t}_1 \tilde{t}_1$	CDF	c-jets+ E_T	0.163	7457 [36]		
$\rightarrow \tilde{\chi}_1^0 c \tilde{\chi}_1^0 c$	DØ	c-jets+ E_T			1.0	0803.2263 [38]
	CDF	c-jets+ E_T			2.6	9834 [39]
$\tilde{t}_1 \tilde{t}_1$	DØ	$b\bar{b}\mu\mu + E_T$	0.339	4866 [45]		
$\rightarrow \tilde{\chi}_1^+ b \tilde{\chi}_1^+ b$	DØ	$b\bar{b}ee(e\mu) + E_T$			1.0	0811.0459 [46]
$\rightarrow \tilde{\nu}\ell^+ b \tilde{\nu}\ell^+ b$	DØ	$b\bar{b}e\mu + E_T$			5.4	1009.5950 [48]
	CDF	$b\bar{b}ee(e\mu)(\mu\mu) + E_T$			1.0	1009.0266 [47]
	DØ	$b\bar{b}\mu\tau(\tau\tau) + E_T$			7.3	1202.1978 [49]
$\tilde{b}_1 \tilde{b}_1$	DØ	$b\bar{b} + E_T$	0.31	4832 [52]		
$\rightarrow \tilde{\chi}_1^0 b \tilde{\chi}_1^0 b$	DØ	$b\bar{b} + E_T$			5.2	1005.2222 [55]
	CDF				2.65	1005.3600 [54]
$\tilde{\chi}_1^+ \tilde{\chi}_1^-$	DØ	“heavy $\mu\mu$ ”	0.390	4746 [59]		
	DØ	“heavy $\mu\mu$ ”			5.2	1110.3302 [60]
	DØ	“heavy $\mu\mu$ ”			6.3	1211.2466 [61]
$\tilde{t}_1 \tilde{t}_1$	CDF	“heavy $\mu\mu$ ”			1.0	0902.1266 [62]

Conflicts of Interest

The author declares no conflict of interest.

References and Notes

1. Fermilab Operations. Available online: <http://www-bdnew.fnal.gov/operations/lum/lum.html> (accessed on 30 December 2013).
2. As the LHC results are continuously being updated, for an up-to-date status of the LHC search results for supersymmetric particles, the reader is referred to the webpages of the ATLAS (<https://twiki.cern.ch/twiki/bin/view/AtlasPublic>) and CMS (<http://cms.web.cern.ch/org/cms-papers-and-results>) collaborations.
3. DØ Collaboration. Search for Squarks and Gluinos in the Jet + Missing E_T Topology. Available online: <http://www-d0.fnal.gov/Run2Physics/WWW/results/prelim/NP/N31/N31.pdf> (accessed on 13 March 2014).
4. DØ Collaboration. Search for squarks and gluinos in events with jets and missing transverse energy in $p\bar{p}$ collisions at $\sqrt{s} = 1.96$ TeV. *Phys. Lett. B* **2006**, *638*, 119–127. doi:10.1016/j.physletb.2006.05.030.
5. CDF Collaboration. Large H_t Event, 2005. Available online: <http://www-cdf.fnal.gov/physics/exotic/exotic.html> (accessed on 30 December 2013).
6. LEP Supersymmetry Working Group (ALEPH, DELPHI, L3 and OPAL Collaborations). LEPSUSYWG, ALEPH, DELPHI, L3 and OPAL experiments, note LEPSUSYWG/04-07.1 (2004). Available online: <http://lepsusy.web.cern.ch> (accessed on 30 December 2013).
7. CDF Collaboration. Search for New Physics in Diphoton Events in $p\bar{p}$ Collisions at $\sqrt{s} = 1.8$ TeV. *Phys. Rev. Lett.* **1998**, *81*, 1791–1796. doi:10.1103/PhysRevLett.81.1791.
8. DØ Collaboration. Search for Supersymmetry with Gauge-Mediated Breaking in Diphoton Events at DØ. *Phys. Rev. Lett.* **2005**, *94*, 041801. doi:10.1103/PhysRevLett.94.041801.
9. CDF Collaboration. Search for anomalous production of diphoton events with missing transverse energy at CDF and limits on gauge-mediated supersymmetry-breaking models. *Phys. Rev. D* **2005**, *71*, 031104. doi:10.1103/PhysRevD.71.031104.
10. CDF and DØ Collaborations. Combination of CDF and DØ Limits on a Gauge Mediated SUSY Model Using Diphoton and Missing Transverse Energy Channel. Available online: <http://arxiv.org/abs/hep-ex/0504004> (accessed on 13 March 2014).
11. DØ Collaboration. Search for diphoton events with large missing transverse energy in 6.3 fb^{-1} of $p\bar{p}$ collisions at $\sqrt{s} = 1.96$ TeV. *Phys. Rev. Lett.* **2010**, *105*, 221802. doi:10.1103/PhysRevLett.105.221802.
12. CDF Collaboration. Search for Supersymmetry with Gauge-Mediated Breaking in Diphoton Events with Missing Transverse Energy at CDF II. *Phys. Rev. Lett.* **2010**, *104*. doi:10.1103/PhysRevLett.104.011801.
13. CDF Collaboration, Search for Heavy Long-Lived particles that Decay to Photons at CDF II. *Phys. Rev. Lett.* **2007**, *99*. doi:10.1103/PhysRevLett.99.121801.
14. CDF Collaboration. The Search For New Physics in the Exclusive $\gamma_{\text{delayed}} + \cancel{E}_T$ Signature in $p\bar{p}$ Collisions at $\sqrt{s} = 1.96$ TeV. Available online: http://www-cdf.fnal.gov/physics/exotic/r2a/20121006.delayedphoton/CDF_Exclusive_GMet_PublicNote_2012.pdf (access on 13 March 2014).

15. DØ Collaboration. Search for the Associated Production of Chargino and Neutralino in Final States with Three Leptons involving τ Leptons. Available online: <http://www-d0.fnal.gov/Run2Physics/WWW/results/prelim/NP/N30/N30.pdf> (accessed on 13 March 2014).
16. DØ Collaboration. Search for the Associated Production of Charginos and Neutralinos in the $e+\tau(\text{had})+\ell$ Final State. Available online: <http://www-d0.fnal.gov/Run2Physics/WWW/results/prelim/NP/N28/N28.pdf> (accessed on 13 March 2014).
17. DØ Collaboration. Search for the Associated Production of Chargino and Neutralino in the $\mu+\tau(\text{had})+\ell$ Final State. Available online: <http://www-d0.fnal.gov/Run2Physics/WWW/results/prelim/NP/N29/N29.pdf> (accessed on 13 March 2014).
18. DØ Collaboration. Search for Supersymmetry via Associated Production of Charginos and Neutralinos in Final States with Three Leptons. *Phys. Rev. Lett.* **2005**, *95*, 151805. doi:10.1103/PhysRevLett.95.151805.
19. DØ Collaboration. Tri-Lepton Expectations (2005). Available online: http://www.fnal.gov/directorate/program_planning/studies/projections09_06_05.htm (accessed on 30 December 2013).
20. DØ Collaboration. Search for associated production of charginos and neutralinos in the trilepton final state using 2.3 fb^{-1} of data. *Phys. Lett. B* **2009**, *680*, 34–43. doi:10.1016/j.physletb.2009.08.011.
21. CDF Collaboration. Search for Supersymmetry in $p\bar{p}$ Collisions at $\sqrt{s} = 1.96 \text{ TeV}$ Using the Trilepton Signature of Chargino-Neutralino Production. *Phys. Rev. Lett.* **2008**, *101*, 251801. doi:10.1103/PhysRevLett.101.251801.
22. CDF Collaboration. Search for trilepton new physics and chargino-neutralino production at the Collider Detector at Fermilab. Available online: http://www-cdf.fnal.gov/physics/exotic/r2a/20110826.trilepton_6fb/cdf10636.pdf (accessed on 13 March 2014).
23. CDF Collaboration. Search for Chargino-Neutralino Associated Production in Dilepton Final States with Tau Leptons. Available online: http://www-cdf.fnal.gov/physics/exotic/r2a/20110809_sstau/Home_files/cdf10611_susy_dilepton_tau.pdf (accessed on 13 March 2014).
24. CDF Collaboration. Search for Supersymmetry with Like-Sign Lepton-Tau Events at CDF. *Phys. Rev. Lett.* **2013**, *110*, 201802. doi:10.1103/PhysRevLett.110.201802.
25. Barger, V.; Wagner, C.E.M.; *et al.* Report of the SUGRA Working Group for Run II of the Tevatron. Available online: <http://arxiv.org/abs/hep-ph/0003154> (accessed on 13 March 2014).
26. DØ Collaboration. Search for squarks and gluinos in events with jets and missing transverse energy using 2.1 fb^{-1} of $p\bar{p}$ collision data at $\sqrt{s} = 1.96 \text{ TeV}$. *Phys. Lett. B* **2008**, *660*, 449–457. doi:10.1016/j.physletb.2008.01.042.
27. CDF Collaboration. Inclusive Search for Squark and Gluino Production in $p\bar{p}$ Collisions at $\sqrt{s} = 1.96 \text{ TeV}$. *Phys. Rev. Lett.* **2009**, *102*, 121801. doi:10.1103/PhysRevLett.102.121801.
28. UA1 Collaboration. Events with Large Missing Transverse Energy at the CERN Collider: III. Mass Limits on Supersymmetric Particles. *Phys. Lett. B* **1987**, *198*, 261–270. doi:10.1016/0370-2693(87)91509-7.
29. UA2 Collaboration. A search for squark and gluino production at the CERN pp Collider. *Phys. Lett. B* **1990**, *235*, 363–372. doi:10.1016/0370-2693(90)91980-P.

30. DØ Collaboration. Search for Squarks and Gluinos in $p\bar{p}$ Collisions at $\sqrt{s} = 1.8$ TeV. *Phys. Rev. Lett.* **1995**, *75*, 618–623. doi:10.1103/PhysRevLett.75.618.
31. DØ Collaboration. Search for Squarks and Gluinos in Events Containing Jets and a Large Imbalance in Transverse Energy. *Phys. Rev. Lett.* **1999**, *83*, 4937–4942. doi:10.1103/PhysRevLett.83.4937.
32. CDF Collaboration. Search for Gluinos and Scalar Quarks in $p\bar{p}$ Collisions at $\sqrt{s} = 1.8$ TeV Using the Missing Energy plus Multijets Signature. *Phys. Rev. Lett.* **2002**, *88*, 041801. doi:10.1103/PhysRevLett.88.041801.
33. ALEPH Collaboration. Search for scalar quarks in e^+e^- collisions at \sqrt{s} up to 209 GeV. *Phys. Lett. B* **2002**, *537*, 5–20. doi:10.1016/j.physletb.2012.02.054.
34. L3 Collaboration. Search for scalar leptons and scalar quarks at LEP. *Phys. Lett. B* **2004**, *580*, 37–49. doi:10.1016/j.physletb.2003.10.010.
35. LEP SUSY Working Group (ALEPH, DELPHI, L3 and OPAL Collaborations). Interpretation of the Results in Minimal SUGRA. Note LEPSUSYWG/02-06.2 (2002). Available online: <http://lepsusy.web.cern.ch> (accessed on 30 December 2013).
36. CDF Collaboration. Search for Direct Pair Production of Scalar Top Quark in $p\bar{p}$ Collisions at 1.96 TeV. Available online: http://www-cdf.fnal.gov/physics/exotic/r2a/20041028.stop_ccmet/cdf7457_stop_c_chi01_pub.pdf (accessed on 13 March 2014).
37. Tevatron Run II Physics Projections (Summer 2005). The Case for Run-II: Submission to the Particle Physics Project Prioritization Panel. The CDF and DØ Experiments. Available online: <http://www-cdf.fnal.gov/physics/projections> (accessed on 30 December 2013).
38. DØ Collaboration. Search for scalar top quarks in the acoplanar charm jets and missing transverse energy final state in $p\bar{p}$ collisions at $\sqrt{s} = 1.96$ TeV. *Phys. Lett. B* **2008**, *665*, 1–8. doi:10.1016/j.physletb.2008.05.037.
39. CDF Collaboration. Search for scalar top decaying into $c+\tilde{\chi}^0$ in the MET+jets sample. Available online: www-cdf.fnal.gov/physics/exotic/r2a/20090709.stop_charm/public_note/publicnote_stop_jul09_v02.ps (accessed on 13 March 2014).
40. Carena, M.; Finch, A.; Freitas, A.; Milstène, C.; Nowak, H.; Sopczak, A. Analyzing the Scalar Top Co-Annihilation Region at the ILC. *Phys. Rev. D* **2005**, *72*, 115008. doi:10.1103/PhysRevD.72.115008.
41. Freitas, A.; Milstène, C.; Schmitt, M.; Sopczak, A. A method for the precision mass measurement of the stop quark at the International Linear Collider. *JHEP* **2008**, *09*, 076. doi:10.1088/1126-6708/2008/09/076.
42. LEP SUSY Working Group (ALEPH, DELPHI, L3 and OPAL Collaborations). Combined LEP Stop and Sbottom Results 183-208 GeV. Note LEPSUSYWG/04-02.1 (2004). Available online: <http://lepsusy.web.cern.ch> (accessed on 30 December 2013).
43. CDF Collaboration. Search for Direct Pair Production of Supersymmetric Top and Supersymmetric Bottom Quarks in $p\bar{p}$ Collisions at $\sqrt{s} = 1.96$ TeV. *Phys. Rev. D* **2007**, *76*, 072010. doi:10.1103/PhysRevD.76.072010.

44. DØ Collaboration. Search for the pair production of scalar top quarks in the acoplanar charm jet topology in $p\bar{p}$ collisions at $\sqrt{s} = 1.96$ TeV. *Phys. Lett. B* **2007**, *645*, 119–127. doi:10.1016/j.physletb.2006.12.024.
45. DØ Collaboration. Search of the lightest scalar top $\tilde{t}_1\tilde{t}_1 \rightarrow b\bar{b}\mu^+\mu^-\tilde{\nu}\tilde{\nu}$ decays at DØ. Available online: <http://www-d0.fnal.gov/Run2Physics/WWW/results/prelim/NP/N35/N35.pdf> (accessed on 13 March 2014).
46. DØ Collaboration. Search for the lightest scalar top quark in events with two leptons in $p\bar{p}$ collisions at $\sqrt{s} = 1.96$ TeV. *Phys. Lett. B* **2009**, *675*, 289–296. doi:10.1016/j.physletb.2009.04.039.
47. CDF Collaboration. Search for the Supersymmetric partner of the top quark in $p\bar{p}$ collisions at $\sqrt{s} = 1.96$ TeV. *Phys. Rev. D* **2010**, *82*, 092001. doi:10.1103/PhysRevD.82.092001.
48. DØ Collaboration. Search for pair production of the scalar top quark in the electron+muon final state. *Phys. Lett. B* **2011**, *696*, 321–327. doi:10.1016/j.physletb.2010.12.052.
49. DØ Collaboration. Search for pair production of the scalar top quark in muon+tau final states. *Phys. Lett. B* **2012**, *710*, 578–586. doi:10.1016/j.physletb.2012.03.028.
50. DØ Collaboration. Search for 3- and 4-body decays of the scalar top quark in $p\bar{p}$ collisions at $\sqrt{s} = 1.8$ TeV. *Phys. Lett. B* **2004**, *581*, 147–155. doi:10.1016/j.physletb.2003.12.001.
51. Nakamura, K. Review of particle physics. *J. Phys. G* **2010**, *37*, 075021. doi:10.1088/0954-3899/37/7A/075021.
52. DØ Collaboration. Search for Direct Production of Scalar Bottom Quarks with the DØ Detector in $p\bar{p}$ Collisions at $\sqrt{s} = 1.96$ TeV. Available online: <http://www-d0.fnal.gov/Run2Physics/WWW/results/prelim/NP/N34/N34.pdf> (accessed on 13 March 2014).
53. DØ Collaboration. Search for pair production of scalar bottom quarks in $p\bar{p}$ collisions at $\sqrt{s} = 1.96$ -TeV. *Phys. Rev. Lett.* **2006**, *97*, 171806. doi:10.1103/PhysRevLett.97.171806.
54. CDF Collaboration. Search for the Production of Scalar Bottom Quarks in $p\bar{p}$ collisions at $\sqrt{s} = 1.96$ TeV. *Phys. Rev. Lett.* **2010**, *105*, 081802. doi:10.1103/PhysRevLett.105.081802.
55. DØ Collaboration. Search for scalar bottom quarks and third-generation leptoquarks in $p\bar{p}$ collisions at $\sqrt{s} = 1.96$ TeV. *Phys. Lett. B* **2010**, *693*, 95–101. doi:10.1016/j.physletb.2010.08.028.
56. DØ Collaboration. Search for the standard-model Higgs boson in the $ZH \rightarrow \nu\bar{\nu}b\bar{b}$ channel in 6.4 fb^{-1} of $p\bar{p}$ collisions at $\sqrt{s} = 1.96$ TeV. Available online: <http://www-d0.fnal.gov/Run2Physics/WWW/results/prelim/HIGGS/H90/H90.pdf> (accessed on 13 March 2014).
57. DØ Collaboration. Updated search for the standard model Higgs boson in the $ZH \rightarrow \nu\bar{\nu}b\bar{b}$ channel in 9.5 fb^{-1} of $p\bar{p}$ collisions at $\sqrt{s} = 1.96$ TeV. Available online: <http://www-d0.fnal.gov/Run2Physics/WWW/results/prelim/HIGGS/H133/H133.pdf> (accessed on 13 March 2014).
58. DØ Collaboration. Search for the standard model Higgs boson in the $ZH \rightarrow \nu\bar{\nu}b\bar{b}$ channel in 9.5 fb^{-1} of $p\bar{p}$ collisions at $\sqrt{s} = 1.96$ TeV. *Phys. Lett. B* **2012**, *716*, 285–293. doi:10.1016/j.physletb.2012.08.034.

59. DØ Collaboration. A Search for Charged Massive Stable Particles at DØ. Available online: <http://www-d0.fnal.gov/Run2Physics/WWW/results/prelim/NP/N27/N27.pdf> (accessed on 13 March 2014).
60. DØ Collaboration. A Search for charged massive long-lived particles. *Phys. Rev. Lett.* **2012**, *108*, 121802. doi:10.1103/PhysRevLett.108.121802.
61. DØ Collaboration. Search for charged massive long-lived particles at $\sqrt{s} = 1.96$ TeV. *Phys. Rev. D* **2013**, *87*, 052011. doi:10.1103/PhysRevD.87.052011.
62. CDF Collaboration. Search for Long-Lived Massive Charged Particles in 1.96 TeV $p\bar{p}$ Collisions. *Phys. Rev. Lett.* **2009**, *103*, 021802. doi:10.1103/PhysRevLett.103.021802.
63. Paige, F.E. SUSY signatures at LHC. In Proceedings of the 10th International Conference on Supersymmetry and Unification of Fundamental Interactions (SUSY'02), Hamburg, Germany, 17–23 June 2002. *Czech. J. Phys.* **2005**, *55*, B185–B196.
64. Sopczak, A. Exploring Supersymmetry at a Future Global e^+e^- Linear Collider. In Proceedings of the Talk at the 11th International Conference on Supersymmetry and Unification of Fundamental Interactions (SUSY'03), Supersymmetry in the Desert, University of Arizona, Tucson, AZ, USA, 5–10 June 2003. Available online: <http://arxiv.org/abs/hep-ph/0403087> (accessed on 13 March 2014).
65. Nojiri, M.M.; Plehn, T.; Polesello, G. Physics Beyond the Standard Model: Supersymmetry. Available online: <http://arxiv.org/abs/0802.3672> (accessed on 13 March 2014).
66. ATLAS Collaboration. Search for Diphoton Events with Large Missing Transverse Momentum in 1 fb^{-1} of 7 TeV proton-proton collision data with the ATLAS detector. *Phys. Lett. B* **2012**, *710*, 519–537. doi:10.1016/j.physletb.2012.02.054.
67. CMS Collaboration. Search for Supersymmetry in Events with Photons and Missing Transverse Energy. CMS-PAS-SUS-12-001, 2012. *JHEP* **2013**, *03*, 111. doi:10.1007/JHEP03(2013)111.
68. CMS Collaboration. Inclusive Search for Supersymmetry Using Razor Variables in pp Collisions at 7 TeV. *Phys. Rev. Lett.* **2013**, *111*, 081802. doi:10.1103/PhysRevLett.111.081802.
69. ATLAS Collaboration. Search for New Phenomena in Final States with Large Jet Multiplicities and Missing Transverse Momentum using $\sqrt{s} = 7$ TeV pp Collisions with the ATLAS Detector. *JHEP* **2011**, *11*, 099. doi:10.1007/JHEP11(2011)099.
70. ATLAS Collaboration. Search for new phenomena in final states with large jet multiplicities and missing transverse momentum at $\sqrt{s} = 8$ TeV proton-proton collisions using the ATLAS experiment. *JHEP* **2013**, *10*, 130. doi:10.1007/JHEP10(2013)130.
71. CMS Collaboration. Search for SUSY using razor variables in events with b-jets in pp collisions at 8 TeV. Available online: <https://cds.cern.ch/record/1596446/files/SUS-13-004-pas.pdf> (accessed on 13 March 2014).
72. CMS Collaboration. Search for top-squark pair production in the single lepton final state in pp collisions at 8 TeV. *Eur. Phys. J. C* **2013**, *73*, 2677. doi:10.1140/epjc/s10052-013-2677-2.